KfK 3331
Mai 1982

Thermal and Mechanical Behaviour of PWR Fuel Rod Simulators for LOCA-Experiments

V. Casal, S. Malang, K. Rust
Institut für Reaktorbauelemente
Projekt Nukleare Sicherheit

Kernforschungszentrum Karlsruhe

KERNFORSCHUNGSZENTRUM KARLSRUHE

Institut für Reaktorbauelemente

Projekt Nukleare Sicherheit

KfK 3331

Thermal and Mechanical Behaviour of PWR Fuel Rod Simulators for LOCA-Experiments

V. Casal, S. Malang, K. Rust

Kernforschungszentrum Karlsruhe GmbH, Karlsruhe

Kernforschungszentrum Karlsruhe GmbH
ISSN 0303-4003

Summary

Performance of the out-of-pile test program REBEKA (reactor typical bundle experiments Karlsruhe) called for prior development of a fuel rod simulator (FRS) whose thermal and mechanical behaviour corresponds largely to that of a nuclear fuel rod during the low-pressure phase of a loss-of-coolant accident (LOCA). To meet this requirement fuel rod simulators with 10.75 mm outer diameter were developed, fabricated,and used in a variety of single rod and several bundle tests.

For new experiments scheduled to provide information about the behaviour of fuel subassemblies having fuel rods with 9.5 mm o.d. quasi-REBEKA FRS's are needed. The thermal and mechanical behaviour of such simulators and of some variants was examined by calculation and compared to that of a fuel rod. Besides the low-pressure phase, the thermal behaviour of some rod types was investigated also at nominal power and in the blowdown phase.

FRS's were designed which simulate almost perfectly fuel rods with respect to the temperatures and deformation of the claddings during low-pressure phase of a LOCA. Some of these FRS's are even suitable for blowdown experiments, if the simulators are operated with a modified decay heat curve.

Zusammenfassung

Thermisches und mechanisches Verhalten von Brennstabsimulatoren für Druckwasserreaktoren für Experimente zum Kühlmittelverluststörfall

Voraussetzung für die Durchführung des out-of-pile Versuchsprogramms REBEKA (reaktortypische Bündelexperimente Karlsruhe) war die Entwicklung eines Brennstabsimulators, (FRS), dessen thermisches und mechanisches Verhalten weitgehend dem eines nuklearen Brennstabes während der Niederdruckphase eines Kühlmittelverluststörfalles entspricht. Für dieses Vorhaben wurden Brennstabsimulatoren mit einem Außendurchmesser von 10,75 mm entwickelt, gefertigt sowie für eine Vielzahl von Einzelstab- und mehrere Bündelversuche verwendet.

Für neu geplante Experimente zum Verhalten von Brennelementen bestehend aus Brennstäben mit 9,5 mm Außendurchmesser werden REBEKA-ähnliche FRS's mit entsprechenden Abmessungen benötigt. Das thermische und mechanische Verhalten solcher Simulatoren und einiger Varianten wurde rechnerisch überprüft und mit dem eines entsprechenden Brennstabes verglichen. Zusätzlich zur Niederdruckphase wurde für einige Stabtypen das thermische Verhalten auch bei nomineller Leistung und der Druckentlastungsphase untersucht.

FRS's wurden ausgelegt, welche Brennstäbe hinsichtlich Hüllrohrtemperaturen und Hüllrohrverformung in der Niederdruckphase eines Kühlmittelverluststörfalles nahezu vollkommen simulieren. Einige dieser FRS's eignen sich sogar für Experimente zur Druckentlastungsphase, wenn die FRS's mit einer modifizierten Nachwärmekurve betrieben werden.

Contents

page

1.	Problem definition	1
2.	Assumptions for calculating the different phases of LOCA	2
2.1	Steady state operation before LOCA	2
2.2	Blowdown	2
2.3	Refill and reflood phases	2
3.	Design of the fuel rod simulators	2
4.	Results	4
4.1	One-dimensional thermal behaviour during the refill and reflood phases	4
4.2	Two-dimensional calculation of the thermal behaviour during the refill and reflood phases	7
4.3	Mechanical behaviour of the Zircaloy cladding during the refill and reflood phases	8
4.4	Thermal behaviour during nominal operation	8
4.5	Thermal behaviour during blowdown	9
5.	Assessment of different fuel rod simulators	11
6.	Feasibility of fuel rod simulators discussed	12
7.	References	13

1. Problem definition

At KfK REBEKA fuel rod simulators (FRS) were developed to simulate the thermal and mechanical behaviour of a KWU-PWR fuel rod during the refill and reflood phases (RR-phases) of a loss-of-coolant accident (LOCA) /1/. REBEKA-FRS's consist of the Zircaloy cladding with KWU dimensions (10,75 mm o.d.) and specifications, an electrical heater rod with boron nitride (BN) as insulating material, and annular Al_2O_3-pellets in the annular gaps between the cladding and the heater rod (Fig. 1). The cosine shaped power profile of the fuel rod is adapted in 7 steps with 4 different power levels by use of heater rods with a tubular conductor with axially variable wall thickness.

Adaption of REBEKA FRS's to a diameter of 9.5 mm o.d. and evaluation of the prospect of applying them to simulate the whole LOCA, beginning with nominal load, and proceeding with blowdown and RR-phases are the subjects of this report. In order to undergo the same clad deformation as a fuel rod, an FRS should meet the following requirements:

- identical transient of the average clad temperature,
- identical azimuthal temperature variation in the cladding.

Both variables are influenced by the thermohydraulics of the steam-water mixture in the coolant channels and by the non-steady state thermal behaviour of the FRS. The thermal and mechanical behaviour of a fuel rod and of different FRS's has been investigated for typical cooling transients.

To calculate the one-dimensional thermal behaviour the HETRAP /2/ computer code was used. For the two-dimensional calculation of temperatures and clad deformation the AZI module from SSYST /3/ was applied.

2. Assumptions for calculating the different phases of LOCA

2.1 Steady state operation before LOCA

- rod power 450 W/cm
- cladding temperature 327 °C

2.2 Blowdown

2.2.1 Blowdown experiments with the rod power adapted to that of the fuel rod

- identical to fuel rod power
- heat transfer coefficient (HTC) during nucleate boiling calculated using Thom's correlation /4/
- transition from nucleate to film boiling with the same delay as in the fuel rod
- HTC during film boiling calculated using Berenson's correlation /5/.

2.2.2 Blowdown experiment with cladding temperature adapted to that of fuel rod

- change of rod power to adjust cladding temperature
- HTC's as in 2.2.1.
- transition from nucleate to film boiling as in 2.2.1.

2.3. Refill and reflood phases

- during refill phase HTC = 30 W/m^2K, coolant temperature 144 °C, system pressure 4.1 bar
- HTC versus time during reflood phase from a FEBA-test (Fig. 2)
- rod power during refill phase changed for the FRS's to achieve a ramp of cladding temperature identical to that of the fuel rod
- rod power of FRS's during reflood phase identical to that of fuel rod.

3. Design of the fuel rod simulators

The dimensions and materials of all FRS's calculated are listed in Table 1. All of them have a Zircaloy with 9,5 mm o.d. The following types of simulators are compared:

- FRS REBEKA-type, dimensions modified,
- FRS REBEKA-type, dimensions modified, Al_2O_3 annular pellets replaced by UO_2-pellets.
- FRS REBEKA-type, dimensions modified, without a filler in the conductor

	Fuel Rod	FRS-No. 1	FRS-No. 2	FRS-No. 3	FRS-No. 4	FRS-No. 5
cladding	Zr-4	Zr-4	Zr-4	Zr-4	Zr-4	Zr-4
outer diameter mm	9.50	9.50	9.50	9.50	9.50	9.50
inner diameter mm	8.36	8.36	8.36	8.36	8.36	8.36
gap width mm	0.03	0.05	0.05	0.05	0.05	0.05
annular pellet	--	Al2O3	Al2O3	UO2	--	--
outer diameter mm	--	8.26	8.26	8.26	--	--
inner diameter mm	--	6.02	5.02	6.02	--	--
gap width mm	--	0.01	0.01	0.01	--	--
heater rod						
cladding	--	Inconel	Inconel	Inconel	Inconel	Inconel
outer diameter mm	--	6.00	5.00	6.00	8.26	8.26
inner diameter mm	--	4.80	4.00	4.80	6.61	6.61
insulator	--	BN	BN	BN	BN	BN
heating source	UO2	Inconel	Inconel	Inconel	Inconel	Inconel
outer diameter mm	8.30	3.50	2.92	3.50	4.82	4.82
inner diameter mm	--	2.97	2.48	2.97	4.09	4.09
filler	--	MgO	MgO	MgO	MgO	--

	FRS-No. 6	FRS-No. 7	FRS-No. 8	FRS-No. 9	FRS-No.10	FRS-No.11
cladding	Zr-4	Zr-4	Zr-4	Zr-4	Zr-4	Zr-4
outer diameter mm	9.50	9.50	9.50	9.50	9.50	9.50
inner diameter mm	8.36	8.36	8.36	8.36	8.36	8.36
gap width mm	0.05	0.01	0.01	0.10	0.20	0.10
annular pellet	Al2O3	Al2O3	--	--	--	--
outer diameter mm	8.26	8.34	--	--	--	--
inner diameter mm	6.02	6.02	--	--	--	--
gap width mm	0.01	0.01	--	--	--	--
heater rod						
cladding	Inconel	Inconel	Inconel	Inconel	Inconel	Inconel
outer diameter mm	6.00	6.00	8.34	8.16	7.96	8.16
inner diameter mm	4.80	4.80	6.61	6.61	6.61	6.61
insulator	BN	BN	BN	BN	BN	BN
heating source	Inconel	Inconel	Inconel	Inconel	Inconel	Inconel
outer diameter mm	3.50	3.50	4.82	4.82	4.82	4.82
inner diameter mm	2.97	2.97	4.09	4.09	4.09	4.09
filler	--	MgO	MgO	MgO	MgO	--

assumed contact coefficients:
Zircaloy - UO2 = 1 W/(cm**2*K)
Inconel - BN = 25 W/(cm**2*K)
Inconel - MgO = 3 W/(cm**2*K)

gaps helium filled (pressure: 60 bar)
heat transmission by conduction and radiation

Table 1: Dimensions and Materials of Fuel Rod and Fuel Rod Simulators

of the internal heater rod.

- FRS without annular pellets and an enlarged diameter of the internal heater rod.
- FRS without annular pellets and an enlarged diameter of the heater rod but without a filler in the conductor of the heater rod.

4. Results

For the calculations with HETRAP code and AZI module materials properties were taken from /6/. But deviating from the data recommended, the density of BN was chosen to be 2.1 g/cm^3 and its thermal conductivity 0.2 W/cm K. All the data of Al_2O_3 heat capacity were multiplied by a factor of 0.9. It was assumed that the gaps in all FRS's in the fuel rod are filled with helium (60 bar). The pressure was kept constant for all calculations and did not vary with temperature and clad deformation. For calculation of heat transmission over the gaps inside the FRS conductivity of the gas and radiation were taken into account. Values of emissivity were chosen which are valid for Zircaloy and Al_2O_3, respectively. For FRS's without annular pellets an emissivity of the heater surface equivalent to that of Al_2O_3 was assumed.

4.1 One-dimensional thermal behaviour during the refill and reflood phases

The range of application of REBEKA-FRS are the RR-phases during a LOCA. Therefore, at first the thermodynamic behaviour of 6 FRS's is discussed for the RR-phases. Then four of them, with the best thermal simulation quality are analysed in addition with respect to clad deformation and to the thermal behaviour during the phases preceding the RR-phases. The design characteristics of 6 FRS's from Table 2 will be discussed in detail below. The conditions prevailing during the RR-phases are plotted versus time in Fig. 2. Time zero is the transition from the refill to the reflood phase. This diagram shows the course of HTC and rod power of the fuel rod and FRS-No. 1. The FRS has a modified rod power in the refill phase (power factor : 1.19) to adjust the ramp of cladding temperature to that of the fuel rod. The basis for this adjustment is the knowledge of HTC during the refill phase. In Table 2 the power factors are listed for FRS's investigated which are necessary to adapt the ramp of the cladding temperature to that of the nuclear fuel rod during the refill phase.

FRS-No.	pellet material	diameter of heater rod (mm)	filler material	power factor
1	Al_2O_3	6	MgO	1.19
2	Al_2O_3	5	MgO	1.20
3	UO_2	6	MgO	1.13
4	no pellet	8.26	MgO	1.19
5	no pellet	8.26	no filler	0.99
6	Al_2O_3	6	no filler	1.08

Table 2: Power factor for FRS during refill phase

A comparison of the power factors does not indicate a significant influence of the annular pellets on the heat capacity. Neither in case of modification of the geometry (FRS's-Nos. 1, 2) nor in case of modification of the material (FRS's-Nos. 1, 3). If the annular pellets are replaced by a heater rod with a greater diameter, the same power factor is required (FRS's-Nos. 1, 4). But, if the filler material in the tubular conductor of the heater rod, inside the FRS's, is replaced by a gas, one gets a significant approximation to the power factor 1. In case of FRS-No. 5 (no annular pellets) the power factor reaches almost unity. In case of FRS-No. 6 (with annular pellets) the power factor is calculated to be 1.08.

Contrary to the refill phase, the rod powers of all FRS's are kept constant and identical to that of the fuel rod during the reflood phase. The reason is the rather small change of cladding temperature during the reflood phase. The ratio of rod power to change in stored heat is much greater than during the refill phase. Deviations in heat capacities therefore influence the cladding temperature at a lower degree. Additionally, the HTC's during reflood phase are varying with time and are dependent from experimental conditions; a change in rod power would be more difficult to realize.

The thermal behaviour of the FRS's discussed is shown in Figs. 3 through 5. The time dependent values of average cladding temperatures, surface heat fluxes, and heat contents are plotted until the point where quenching occurs. The fuel rod and FRS's-Nos. 1 through 6 are considered. A comparison of the different diagrams shows the following trends:

- Surface temperature:
  - FRS's-Nos. 1, 2, 3, 4 show for the turnaround time an almost identical behaviour, deviations up to 24 K from the fuel rod occur.
  - FRS-No. 6 deviates only 10 K.
  - FRS-No. 5 shows an absolutely identical behaviour.

- Surface heat flux:
  - No significant deviation from the fuel rod before quenching occurs.
  - During quenching FRS's-Nos. 1, 2, 3, 4 have an 20 % higher heat flux.
  - FRS-No. 6 shows an 8 % too high heat flux during quenching.
  - FRS-No. 5 shows a behaviour identical to that of the nuclear fuel rod.

- Stored heat:
  - FRS's-Nos 1, 2, 4 deviate by up to 18 %,
  - FRS-No. 3 (UO_2-pellet) by up to 10 %,
  - FRS-No. 6 by up to 6 %
  - FRS-No. 5 identical behaviour.

An assessment of the thermal behaviour can be based upon the course of cladding temperature. Knowledge of the surface heat flux and stored heat helps only its understanding. The course of cladding temperatures during the RR-phases is the dominating condition for clad deformation due to internal overpressure. A deviation by 10 K can result in a significant change of deformation. The FRS's investigated under the conditions discussed show a negligible influence of the dimensions of the annular Al_2O_3-pellets on the thermal behaviour; even if the pellets are replaced by a heater rod with a larger diameter (FRS's-No. 4), the same course of temperature is observed. Pellets of UO_2 (FRS-No. 3) give a slightly better adaptation to the fuel rod. But the improvement is small and does not warrant the necessary implications in case UO_2 would be used in an out-of-pile experiment. An excellent adaptation of the thermal behaviour of fuel rod is reached with FRS-No. 5 which consists of the Zircaloy cladding and a heater rod mounted directly inside the cladding with an empty tubular conductor. Calculations with different internal gaps inside the FRS's were carried out (FRS's-Nos. 7 through 11). No significant deviations of the thermal behaviour were found resulting from the modifications investigated.

4.2 Two-dimensional calculation of the thermal behaviour during the refill and reflood phases

The one-dimensional calculations already discussed show the course of average temperatures. A good thermal correspondence between a fuel rod and an FRS of nominal geometry is a basic requirement but not necessarily a sufficient one. In reality the width of the gas filled gap underneath the Zircaloy cladding will not be constant and uniform. At some axial positions the Zircaloy cladding will be in contact with the annular pellets beneath. At the opposite side the gap width will reach twice its nominal value. This eccentricity will cause local temperature variations of the Zircaloy cladding which will determine essentially the amount of clad strain before rupture. FRS's with their different internal structures may have different local temperature variations, and therefore a different mechanical behaviour in case of an eccentricity. This could be expected especially for FRS's-Nos. 4 and 5 since they have no annular pellets. The Zircaloy claddings of these FRS's are in contact with the metallic sheath of the heater rod. Because of the great difference in thermal conductivities of steel and ceramics (UO_2 or Al_2O_3), one could anticipate in case of eccentricity a different local temperature distribution and, consequently, a different amount of deformation.

To begin with, the results of AZI based calculations of the azimuthal variation of the cladding temperature in the RR-phases without clad deformation are plotted in Fig. 6 as a function of time for the fuel rod and FRS's-Nos. 1, 4, 5; negative time marks the refill phase, positive time marks the reflood phase. One realizes that the azimuthal variation of cladding temperature is lowest for the fuel rod. All FRS's show about 50 % greater variations. All FRS's considered behave almost identically. The following boundary conditions were assumed for the calculations discussed:

- rod power, HTC, and coolant pressure, Fig. 2.
- maximum possible eccentricity, i.e. the pellets or the heater touch the cladding at one side,
- geometry and materials properties equal to those in the calculation with HETRAP.
- fill gas helium

4.3 Mechanical behaviour of the Zircaloy cladding during the refill and reflood phases

The results of calculations with AZI, including clad deformation, are shown in Figs. 7 and 8, again for FRS's-Nos. 1,4,5, and the nuclear fuel rod. A constant internal gas pressure of 60 bar has been used which causes the same cladding stress as in the REBEKA-tests with KWU fuel rod diameter.

The following can be stated:

- During the refill phase the fuel rod undergoes the lowest temperature variation in the cladding (~ 5 K).
- During that period all FRS's undergo approximately the same azimuthal temperature variation (~ 7 K).
- Rupture of the claddings occurs 28 - 36 seconds after beginning of reflood phase; deviations from the fuel rod are 2.5 sec (FRS-No. 1) and 7.4 sec (FRS-No. 5).
- During the reflood phase the azimuthal temperature variation is lowest in case of the fuel rod (10 K after 10 sec); at the same time, all FRS's considered undergo temperature variations of 12 - 13 K.
- The cladding of the fuel rod fails after an average circumferential elongations of 37 %. The corresponding elongation for the claddings of the FRS's are 31 - 32 %.

Cladding strain of fuel rod and FRS's do not deviate to a large extend. However, converted geometrically to a blockage ratio, in case of coplanar strain, the blockage are 70 % for fuel rod and 58 % for FRS's, respectively.

Scoping calculations have shown, that fill gases with lower thermal conductivities lead to a reduction in strain. Therefore a fuel rod with a high burnup may have a even lower cladding strain than a FRS with helium filling. On the other hand a smaller eccentricity would increase the strain.

4.4 Thermal behaviour during nominal operation

Although REBEKA-type FRS's have been developed only for simulation of the RR-phases it will be discussed below whether they could be used to simulate nominal operation of a nuclear fuel rod.

Conditions: - rod power 450 W/cm
- cladding temperatures 327 °C
- internal pressure 60 bar.

The radial temperature profiles are shown in Figs. 9 and 10. It can be stated:

- FRS-No. 1 will reach a conductor temperature of 1250 °C; in case of an increase of the inner gap (heater rod - annular pellet) from 10 µm to 50 µm, caused by tolerances of the annular pellets, the temperature of the conductor will reach 1430 °C.
- FRS-No. 3 with annular UO_2-pellets would have a conductor temperature of 1720 °C.
- FRS's-Nos. 4 and 5: The temperature of the conductor is 880 °C; even an increase of the gap to 100 µm raises the conductor temperature to 1086 °C only.

FRS's with NiCr conductor were operated at KfK with conductor temperatures of 1250 °C for about 10 hours /7/. If tolerances of pellets could be excluded, FRS-No. 1 with an Al_2O_3-pellet could meet the requirement of operating with nominal load for a limited period of time. But the realistic tolerances of the annular pellets exclude this FRS for nominal operation. A reliable operation of nominal load would be possible with FRS's-Nos. 4 and 5.

4.5 Thermal behaviour during blowdown

At the beginning of a LOCA, caused by a large break, a blowdown will occur. For this event the course of coolant pressure and saturation temperature as well as the course of HTC and decay heat of the nuclear fuel rod are plotted in Fig. 11. The transient HTC, especially the transition from nucleate boiling to film boiling, depends on the surface heat flux. The course chosen is valid for nuclear fuel rods. FRS's with a different thermal behaviour will have this transition at a different time which is not taken into account in this calculation. This would result in very different cladding temperatures and heat contents. The starting conditions for the following RR-phases would be very different.

4.5.1 Behaviour of FRS's during blowdown with the rod power identical to the decay heat of the nuclear fuel rod

With the assumptions plotted in Fig. 11 calculations were carried out with

HETRAP to evaluate the thermal behaviour. The results are shown in Figs. 12 and 14. A comparison of the results of these two figures leads to the following conclusion. The heat stored during normal operation is highest for the fuel rod and lowest for FRS-No. 5. This causes during a blowdown too low temperature ramp after DNB for all FRS's compared. Even FRS-No. 1 which is closest to the fuel rod deviates by up to 50 K. None of the FRS's is capable of simulating blowdown when the FRS's are operated with a power transient identical to that of the fuel rod.

4.5.2 Behaviour of FRS's during blowdown with changed rod power

One can improve that simulation quality of the FRS's by variation of the power transient during blowdown /8/ in order to adjust the course of cladding temperature to that of the nuclear fuel rod. Because of the very high HTC's during nucleate boiling and the very low HTC's during film boiling, one gets the best approximation with an adaptation of heat flux during the first phase of blowdown, and with an adaptation of cladding temperature for the following phase. The success of these calculations is shown in Figs. 15 through 20.

The following can be stated:

- Variations of power transients lead to a course of cladding temperatures and heat fluxes better approximating those of the nuclear fuel rod; but identical behaviour is not attained.
- The course of the heat flux of the fuel rod during nucleate boiling can be fitted best for FRS's-Nos. 4 and 5; FRS-No. 1 deviates by up to 10 %.
- The transients of cladding temperatures during nucleate boiling are simulated well by all FRS's discussed.
- The transients of cladding temperatures during film boiling are simulated reasonably with some deviation from the fuel rod.

As a result one can state: If the dependency of HTC on time is known during blowdown, it is possible to adapt the time dependent heat flux of FRS's-Nos. 4 and 5 to that of a nuclear fuel rod. A good simulation of blowdown is then possible. It can be assumed that a similar adaptation to the nuclear fuel rod can be attained, if the courses of rod power (Figs. 16, 18, 20) are smoothed down adequately.

5. Assessment of different fuel rod simulators

FRS's discussed can be adapted in the RR-phase to fuel rods having 9.5 mm o.d. This is possible with both a simulator with annular Al_2O_3-pellets as with one containing only an 8.2 mm heater rod inside the Zircaloy cladding (FRS's-Nos. 1 and 4). Both simulators show the same thermal and mechanical behaviour. A replacement of the Al_2O_3-pellets by UO_2-pellets (FRS-No. 3) shows no significant improvement that would justify the additional effort in handling UO_2-pellets. If the MgO inside the conductor of the heater rod is replaced by a gas-filling (FRS-No. 5), one gets an exact simulation of the thermal behaviour during the RR-phases; only eccentric gaps cause larger temperature variations in the Zircaloy cladding which result in a smaller average circumferential elongation.

The heater rods used inside the FRS's usually have 250 % thermal expansion of the Zircaloy cladding. In the RR-phases, the phase of deformation of Zircaloy, a temperature rise up to 400 °C may occur. This temperature rise causes an axial relative motion between Zircaloy and the heater rod of up to 4 mm per meter of heated length. At least in case of FRS's-Nos. 4 and 5 with their high stability against bending additional forces on the Zircaloy cladding may be imposed during deformation by thermal expansion of the internal heater rod. This effect should be investigated before such FRS's are used in clad deformation experiments.

6. Feasibility of fuel rod simulators discussed

For experimental investigations of a LOCA FRS's-Nos. 1, 4,5 show a suitable behaviour at least for parts of the accident. Important criteria for selection of one FRS are the possibility of its realization, and the amount of experience already available about them.

FRS-No. 1 which is suitable to simulate RR-phases, is the well known REBEKA FRS. Only the dimensions of the Zircaloy cladding and of the Al_2O_3-pellets are modified. With step-wise adaptation of axial power profile, a few hundred FRS's have already been produced and applied in experiments. Because in FRS-No. 1 a heater rod is used with dimensions identical to REBEKA-FRS's, applying them would involve no risk at all. When a continuous approximation of the axial power profile is required, two solutions are available. One set of heater rods for one REBEKA-bundle have been produced already with an continuous variation of the wall thickness of the tubular conductor inside the heater rod. The second design uses a conductor in the form of a helix with variable width of the ribbon. This design offers the advantage of adapting the axial power profile with high accuracy with usual tolerances during fabrication. Heaters of this type were applied in sodium boiling experiments in KfK multi-rod bundle tests. This year one 7-rod bundle with these heaters fabricated by INTERATOM will be installed in the HALDEN-reactor. Until now more than 900 ribbon-type heater rods have been produced at KfK,including 90 with cosine power profiles. Realized heated length go up to 1500 mm, greater lengths can be produced without needing additional development work. Fig. 21 shows the power profile of the FRS's required for HALDEN-reactor and the corresponding width of the ribbon. One notes that large variations of the width are necessary which are easy to machine. Fig. 22 shows a radiograph of a heater rod with cosine power profile. Near the cold end the ribbon has a great width, in the central part the width has its minimum.

FRS-No. 4 (without annular pellets) which is suitable to simulate the whole LOCA, can be produced both with a tubular and a helical conductor. The diameter required (8.2 mm) is in the range already fabricated. FRS's-Nos. 5 and 6 with an empty tubular conductor are more difficult to fabricate. Densification of BN between the heater rod cladding and the conductor is performed at KfK by strong diameter reduction of the heater rod. This strong reduction of diameter offers the significant advantage that heater rods with uniform BN-density are guaranteed. Other production methods cannot avoid the possible formation of local zones with low BN-density. Variations of the BN-density cause unacceptable cold spots on the cladding and, correspondingly inside hot spots on the conductor. The first effect would lead to an unpredictable thermal behaviour of the FRS, the latter to an overheating of the conductor. The KfK production method involving strong reduction in diameter calls for a filled conductor to achieve the forces of reaction during diameter reduction necessary for BN densification. At KfK several prototype-heater rods have been produced with empty tubular conductor using the proved technique of KfK. During fabrication the electrodes were filled, afterwards they were emptied out. Fig. 23 shows photographs of a heater rod with empty electrode and of a normal heater rod whose helical electrode is filled with MgO.

7. References

/1/ F. Erbacher, H. J. Neitzel, M. Reimann, K. Wiehr:
Out-of-pile Experiments on Ballooning in Zircaloy Fuel Rod Claddings in a Low Pressure Phase of a Loss-of-Coolant Accident.
CSNI-Report No. 13, Part 2; Proceedings of Specialist Meeting on the Behaviour of Water Reactor Fuel Elements under Accident Conditions.
Spåting, Norway (13 - 16 Sept. 76).

/2/ S. Malang: HETRAP: A Heat Transfer Analysis Program,
ORNL-TM-4555,(Sept. 74).

/3/ R. Meyder: SSYST - Eingabebeschreibung und Handhabung.
KFK 2966,(Nov. 80).

/4/ J.R. Thom et al.: Booling in Subcooled Water during Flow Up Heated Tubes or Annuli. Proc. Inst. Mech. Eng., Vol. 180, Part 3c,
pp. 226 - 246 (1966).

/5/ P.J. Berenson: Film Boiling Heat Transfer from a Horizontal Plate
ARS-Journal, Vol. 33, pp. 553 (April 62).

/6/ K. Rust, S. Malang, W. Götzmann:
PEW- Ein Fortran-Rechenprogramm zur Bereitstellung physikalischer Eigenschaften von Werkstoffen für LWR-Brennstäbe und deren Simulatoren.
KFK-Ext. 7/76-1,(Dez. 76).

/7/ V. Casal: Design of High-Performance Fuel Pin Simulators for Thermodynamic Experiments with Nuclear Fuel Elements.
Nuclear Technology, Vol. 47,pp. 153-162 (Jan. 80).

/8/ S. Malang: Simulation of Nuclear Fuel Rods by using Process Computer Controlled Power for Indirect Electrically Heated Rods.
ORNL-TM-4712,(Nov. 75).

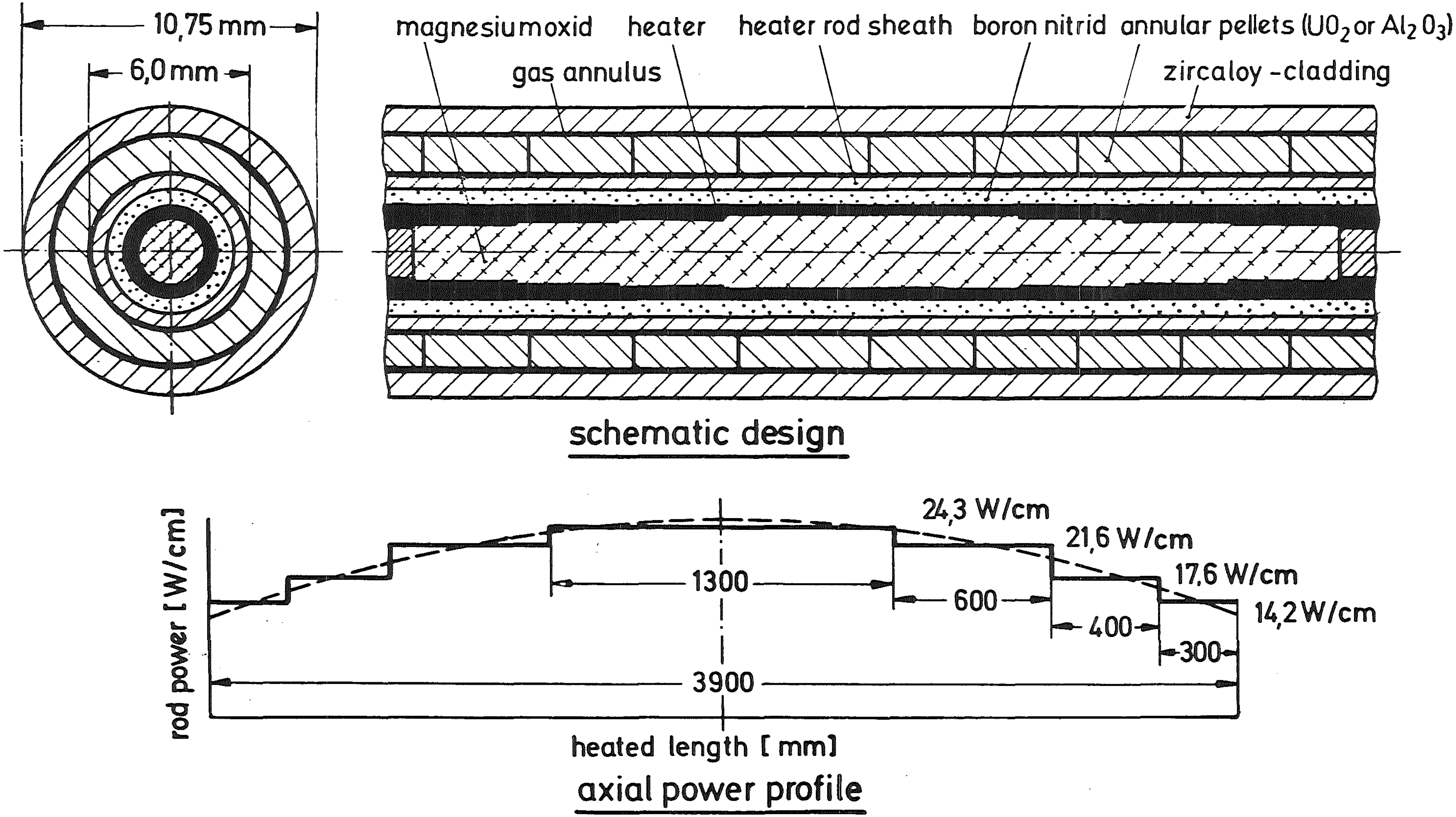

Fig. 1 REBEKA fuel rod simulator

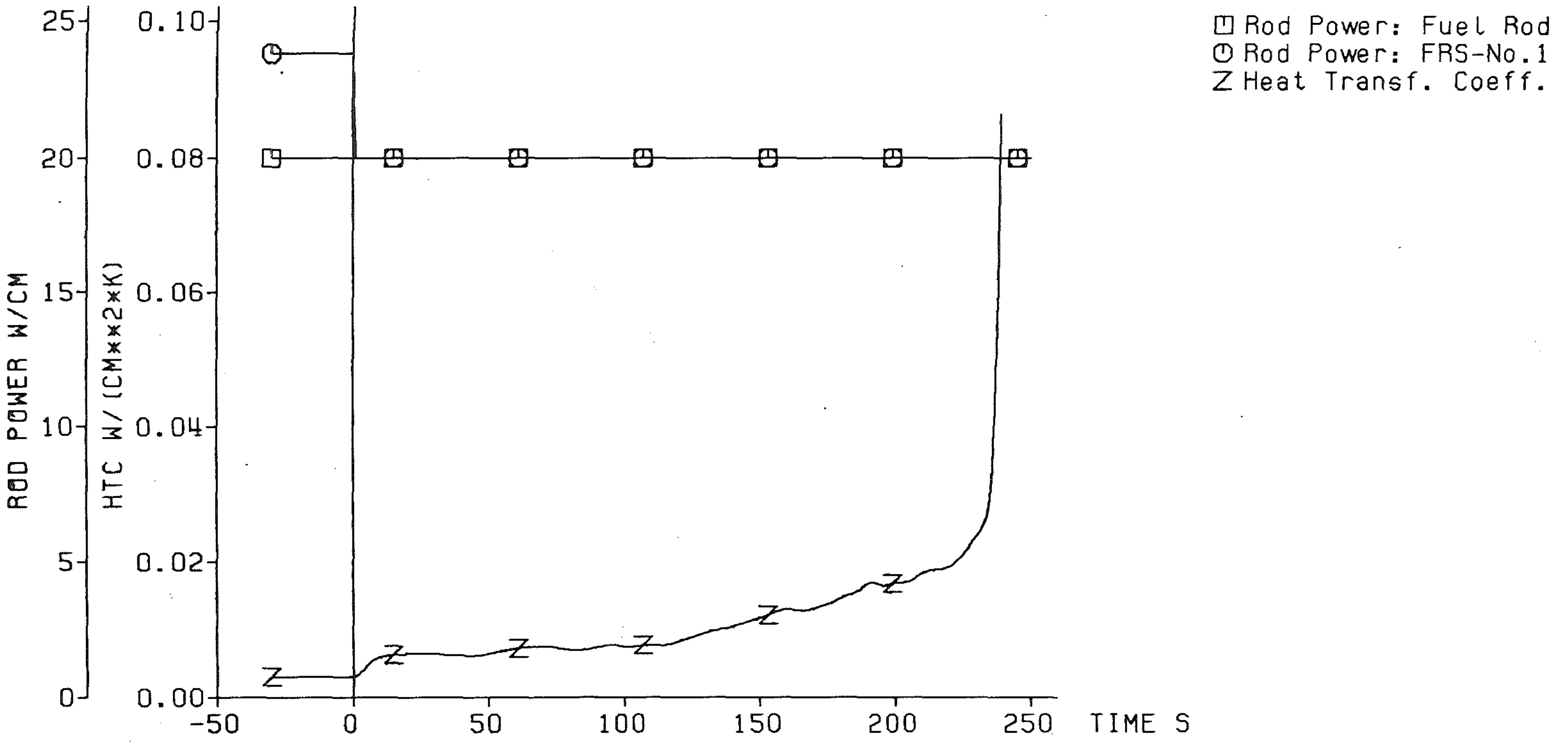

Fig. 2 Rod power and heat transfer coefficient (HTC) during refill and reflood phase

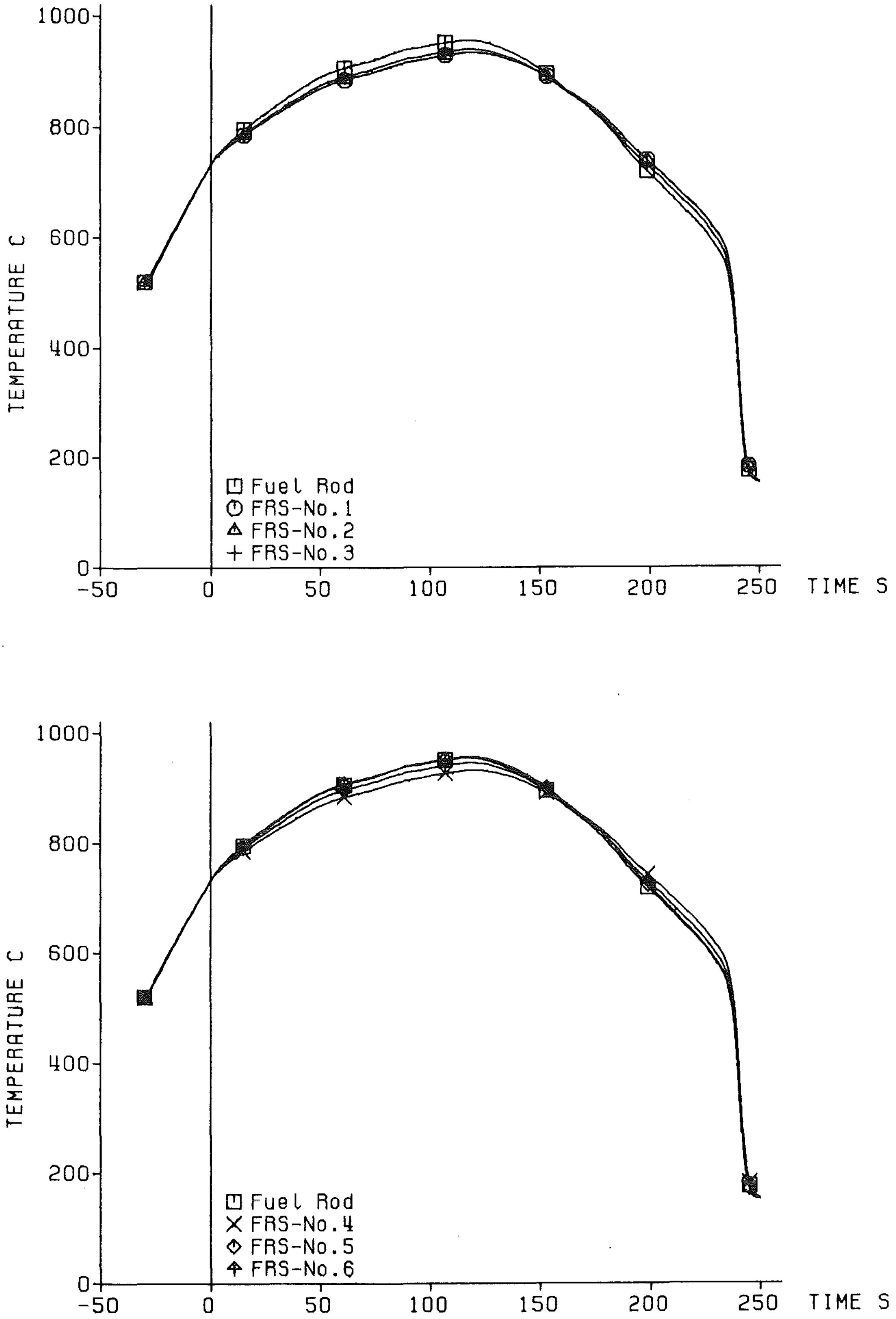

Fig. 3 Cladding temperature during refill and reflood phase

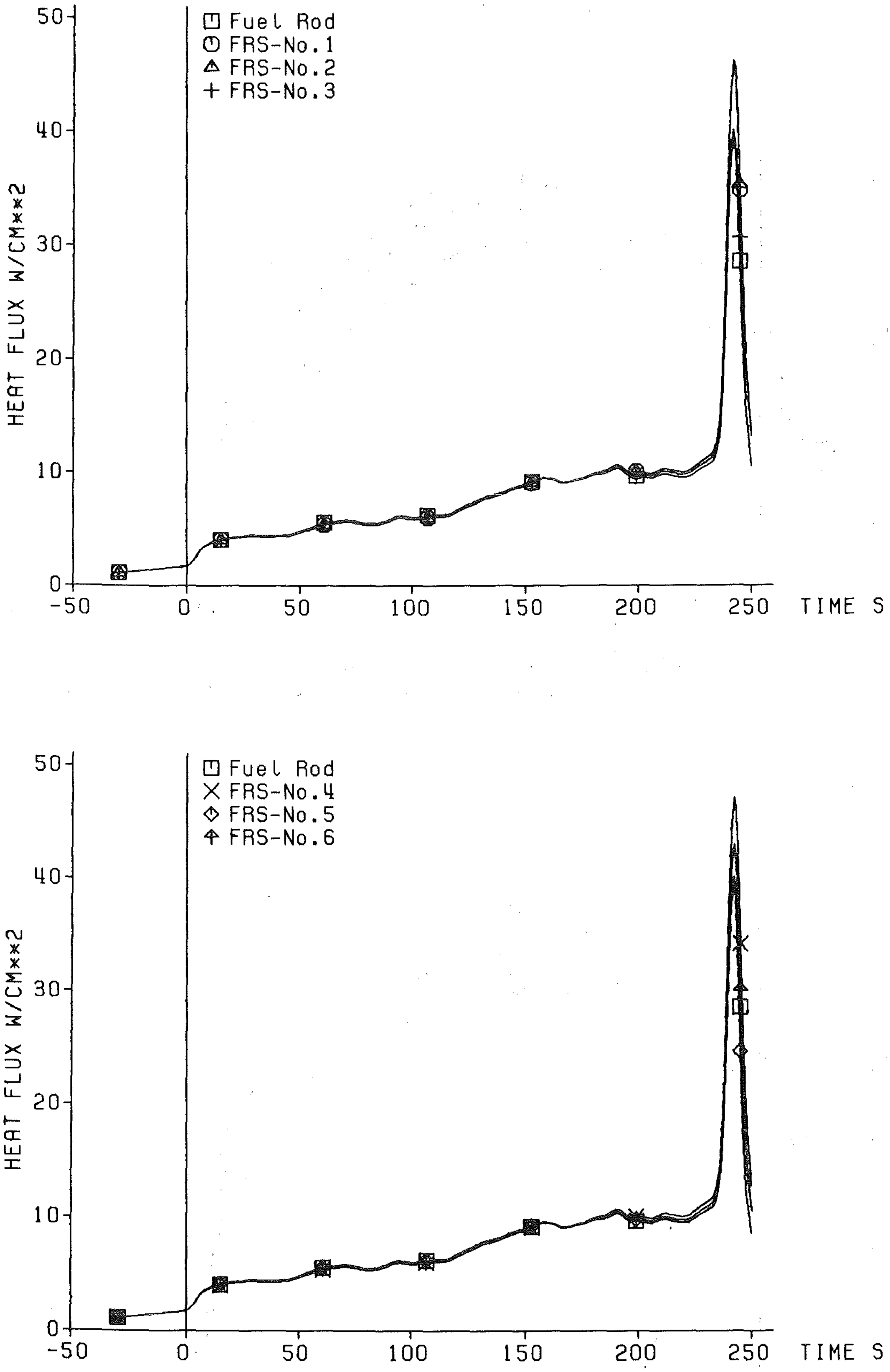

Fig. 4 Surface heat flux during refill and reflood phase

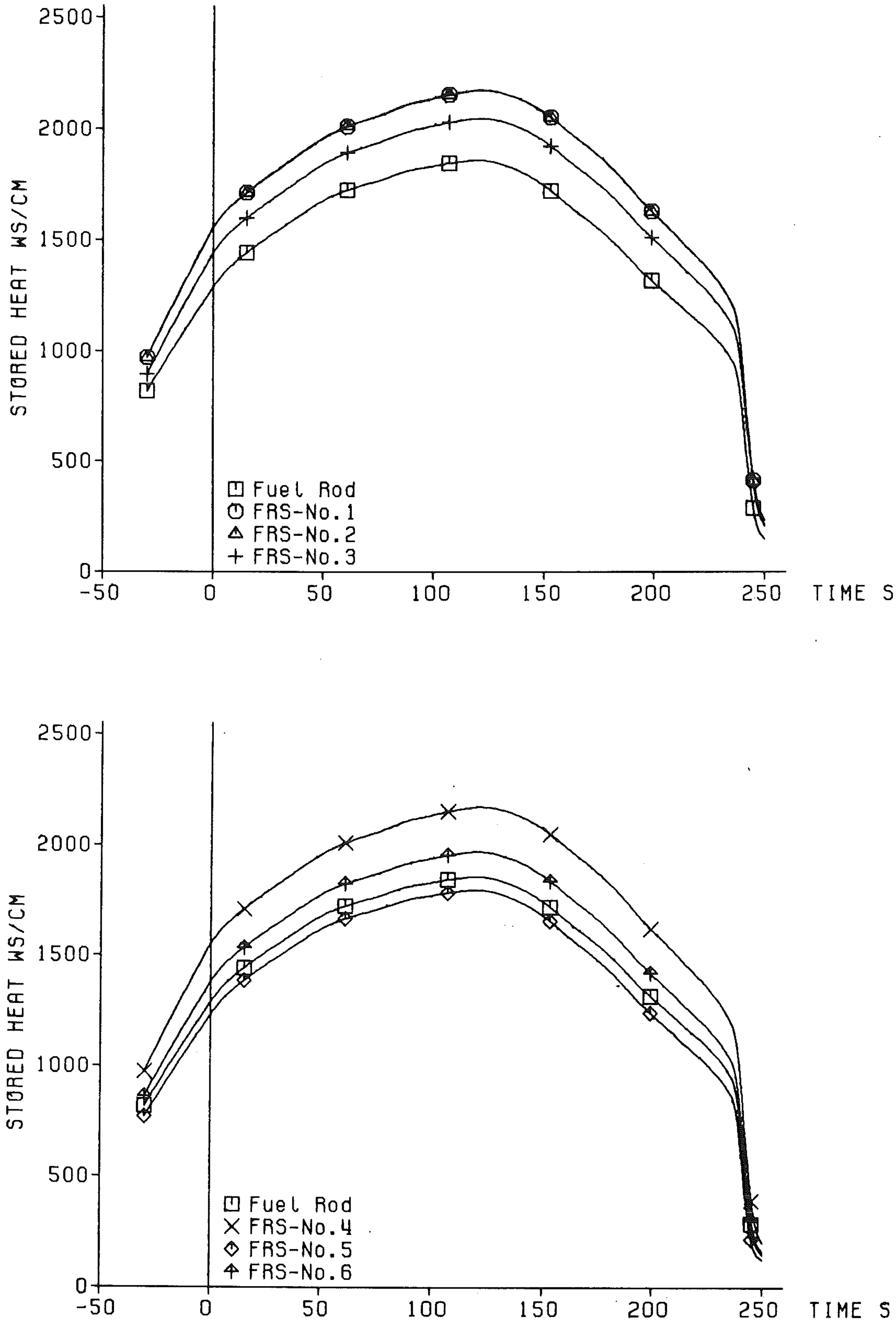

Fig. 5 Stored heat during refill and reflood phase

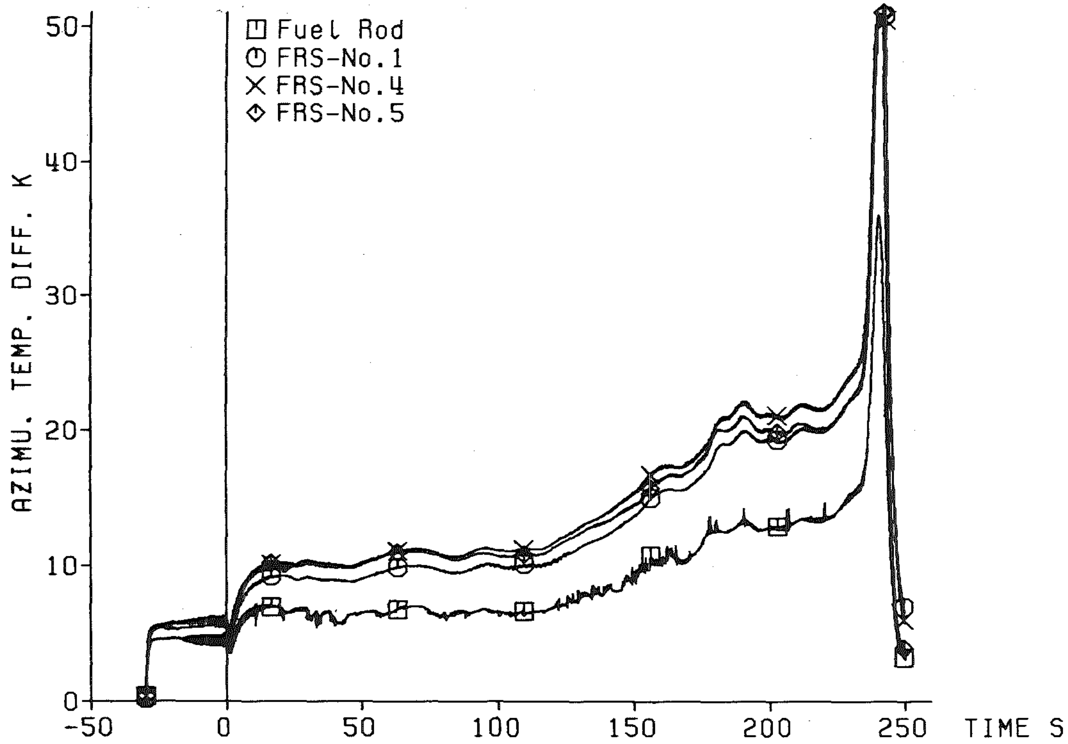

Fig. 6 **Azimuthal cladding temperature variation without clad deformation during refill and reflood phase**

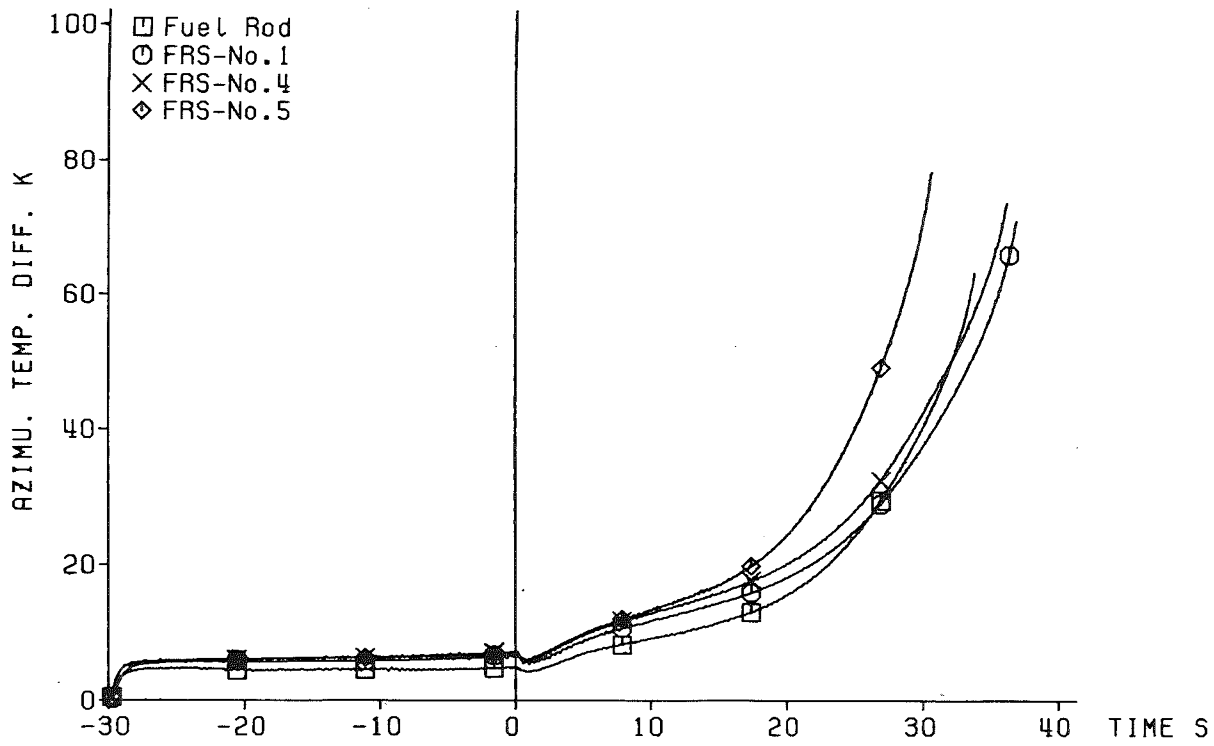

Fig. 7 Azimutal cladding temperature variation with clad deformation during refill and reflood phase

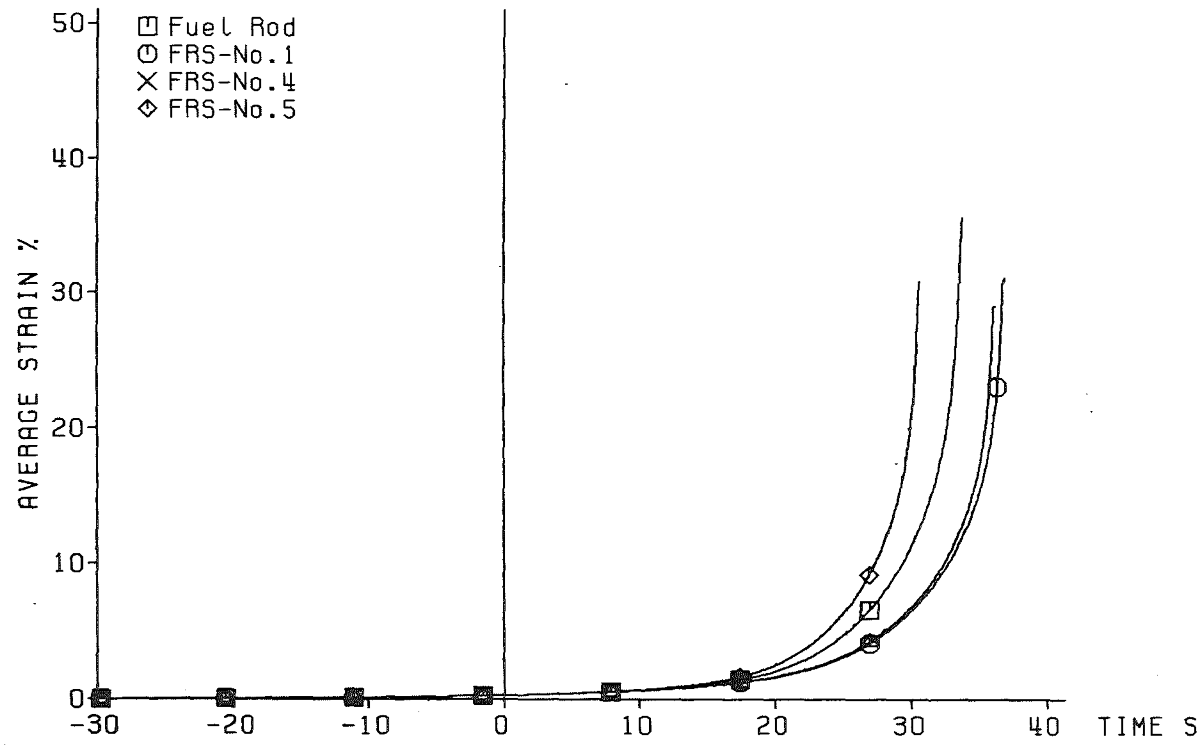

Fig. 8 Average cladding strain during refill and reflood phase

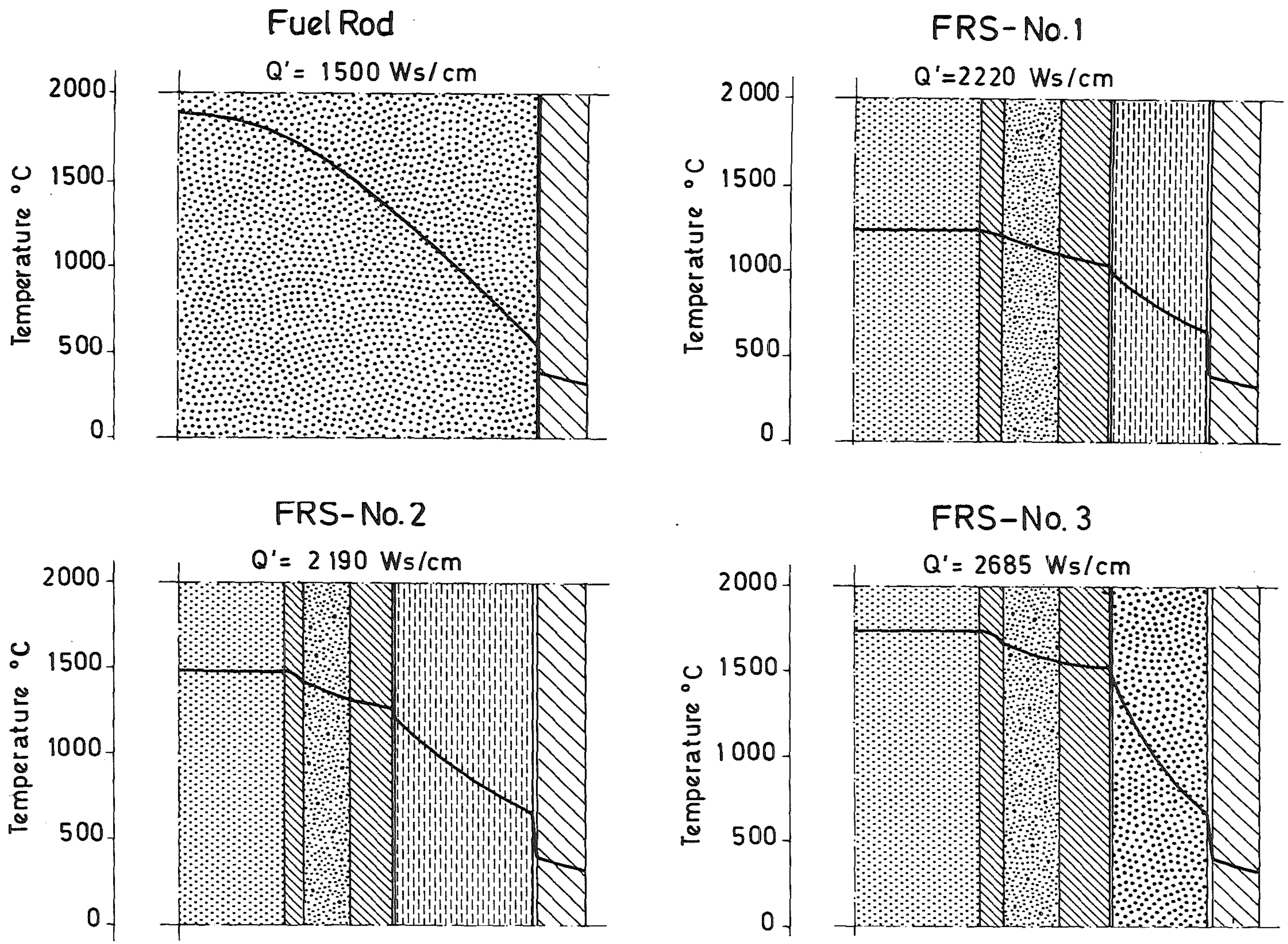

Fig. 9 **Cross section, radial temperature profile, and stored heat Q' during nominal operation**

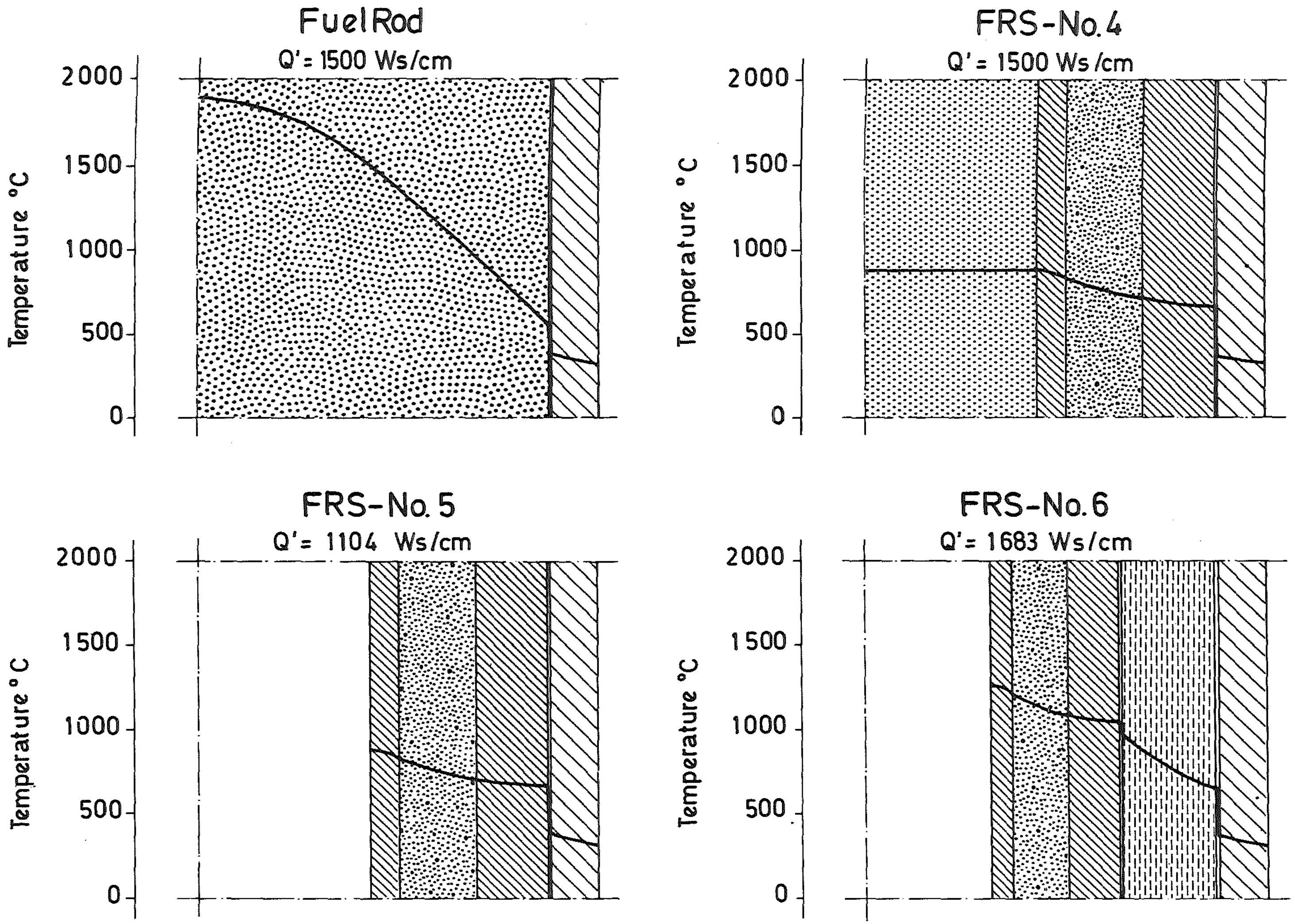

Fig. 10 Cross section, radial temperature profile, and stored heat Q' during nominal operation

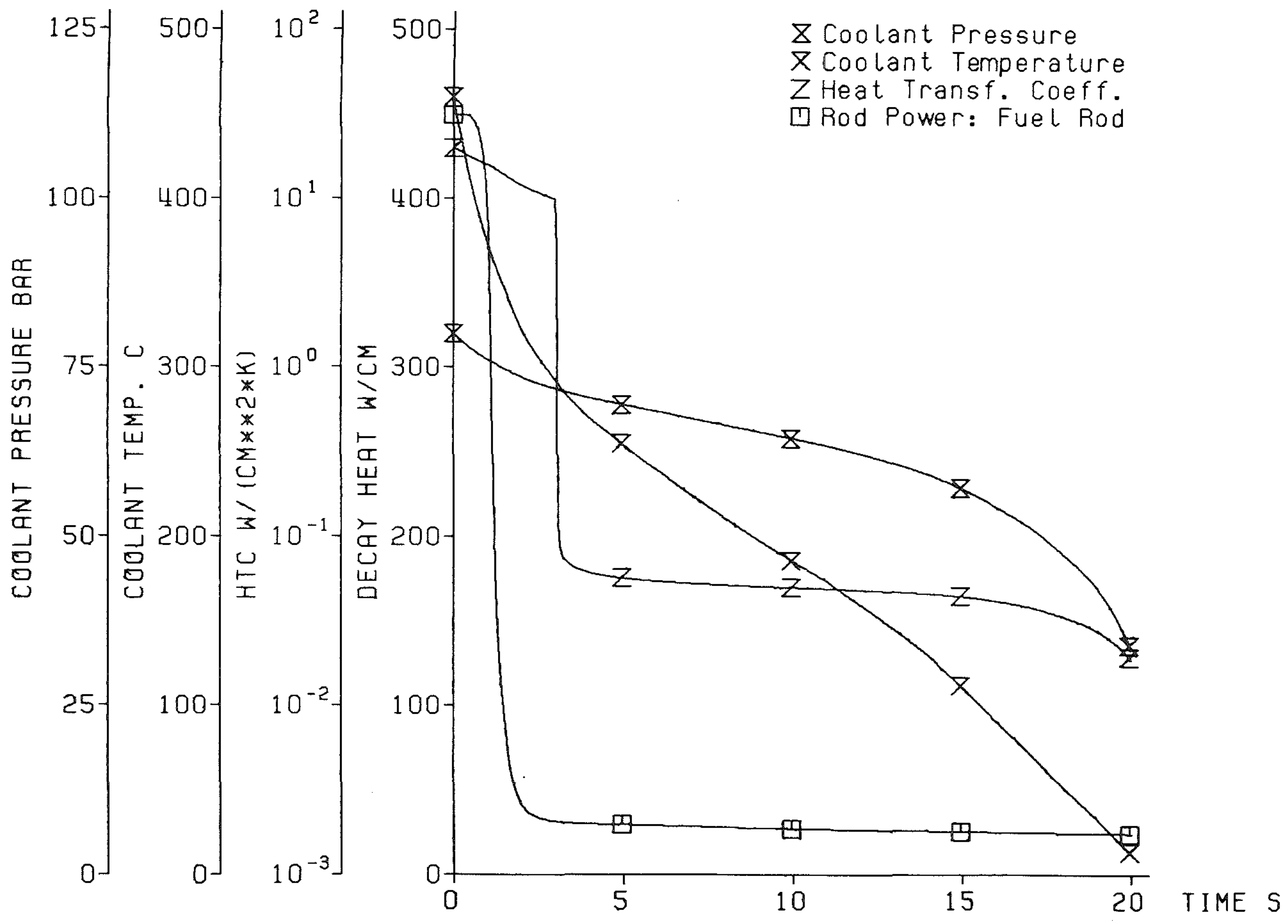

Fig. 11 Boundary conditions for a fuel rod during blowdown phase

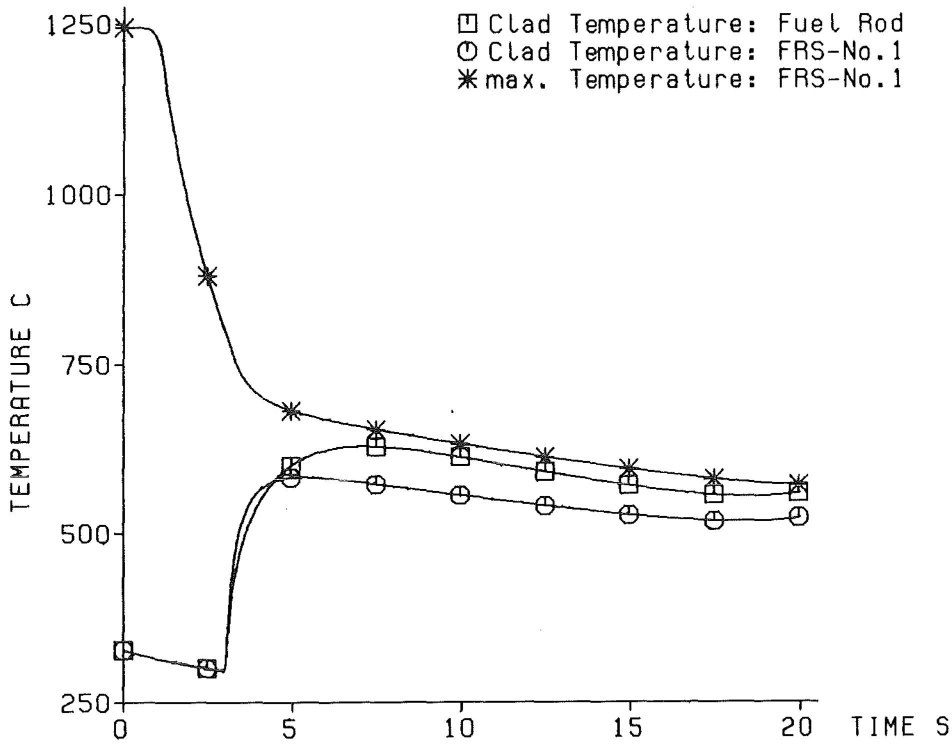

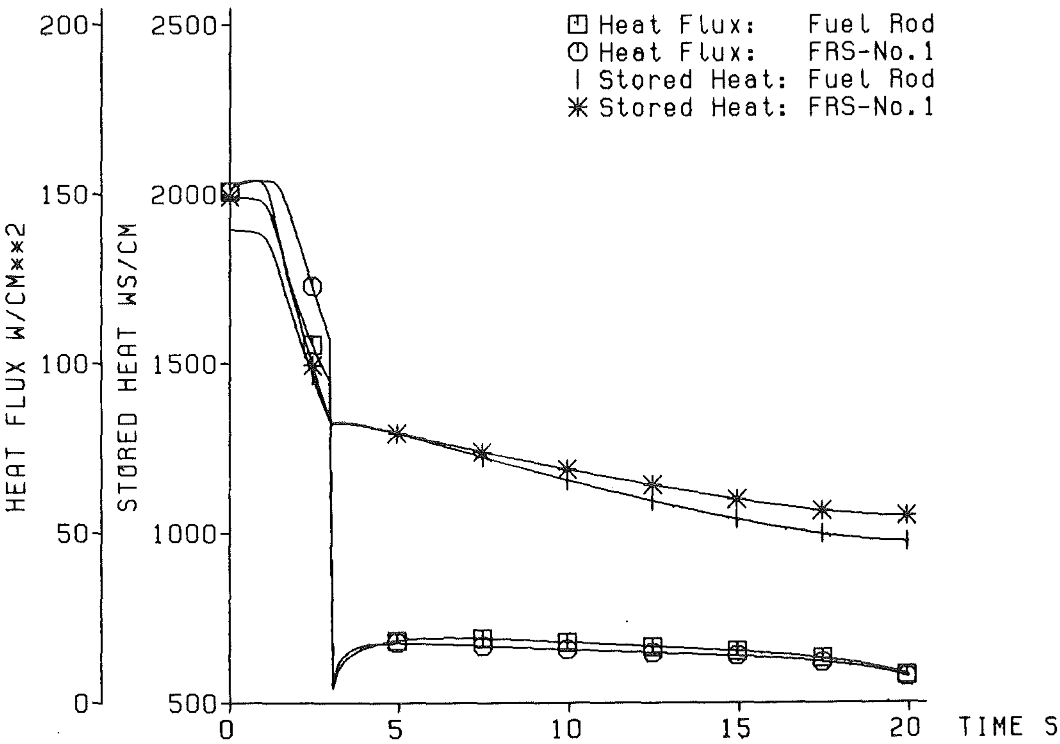

Fig. 12 Thermal behavior of rods under identical boundary conditions during blowdown phase

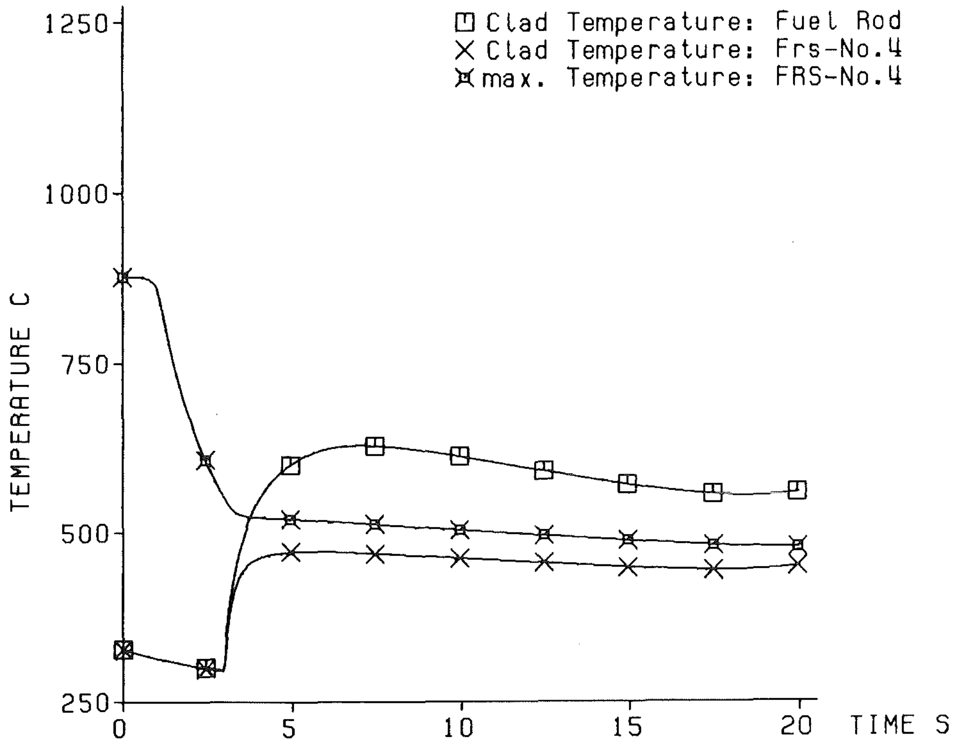

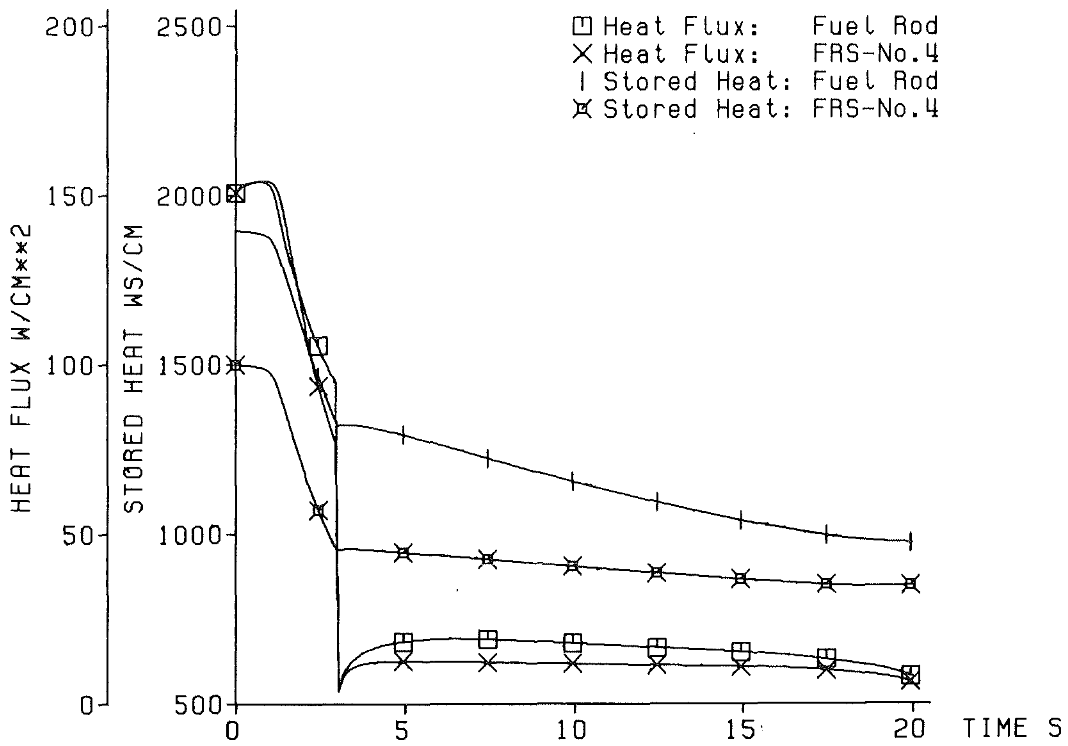

Fig. 13 Thermal behavior of rods under identical boundary conditions during blowdown phase

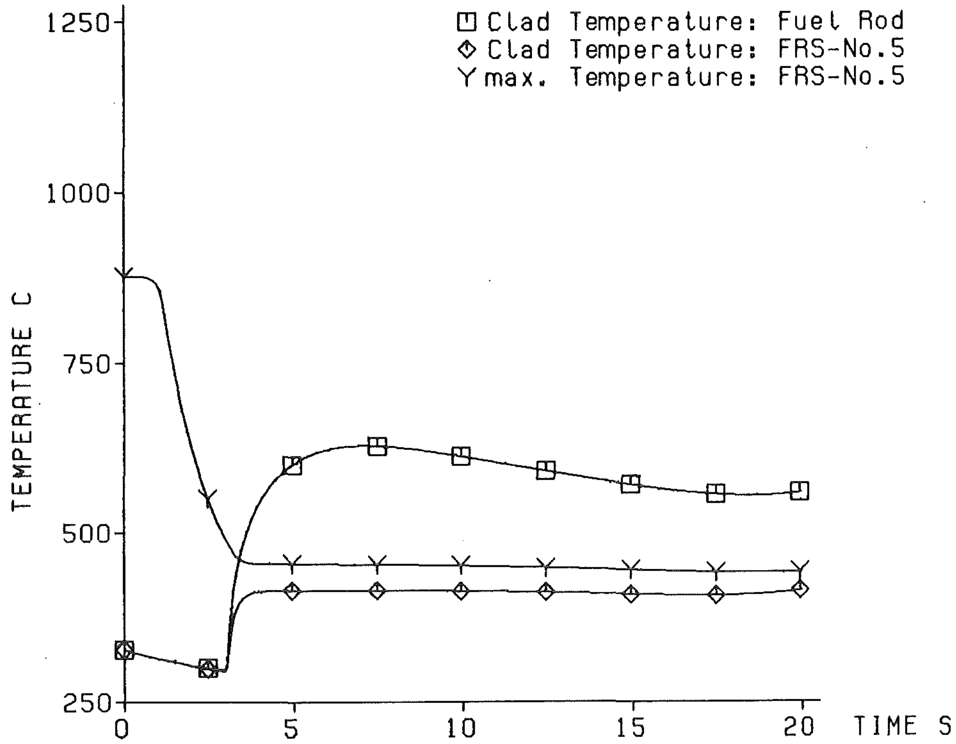

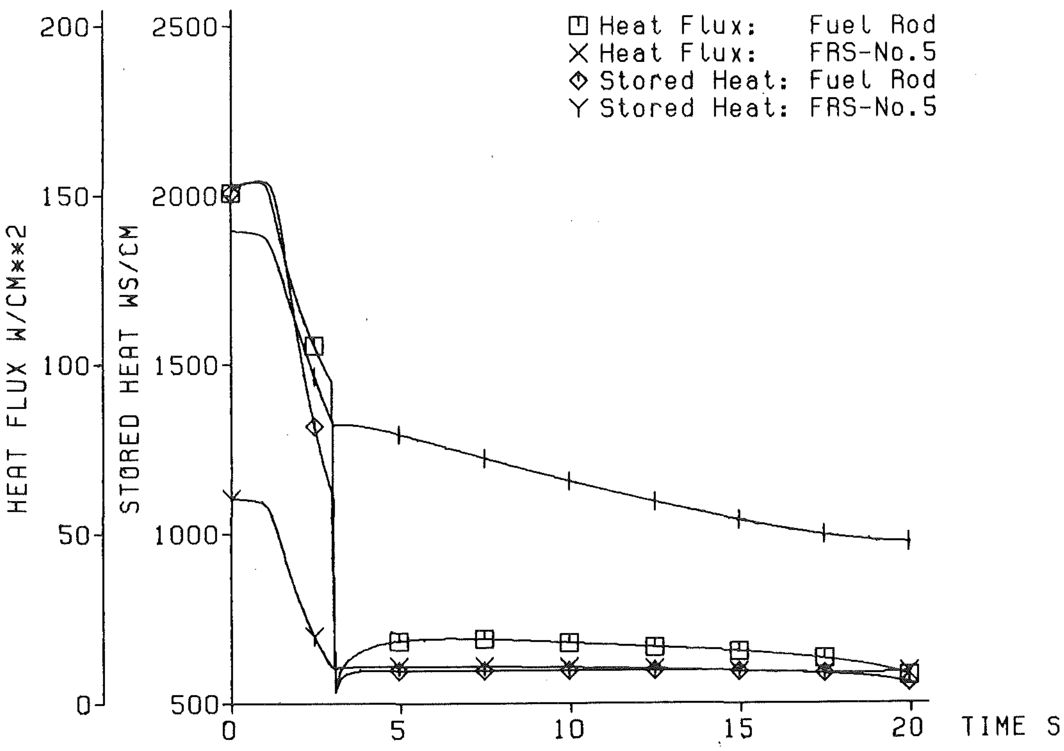

Fig. 14 Thermal behavior of rods under identical boundary conditions during blowdown phase

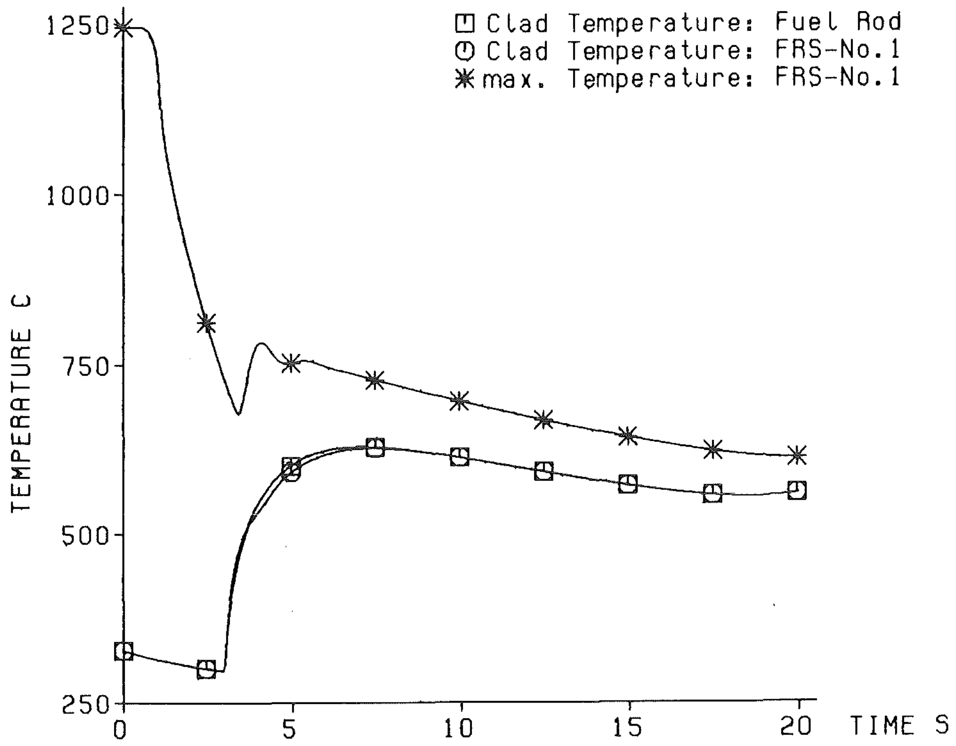

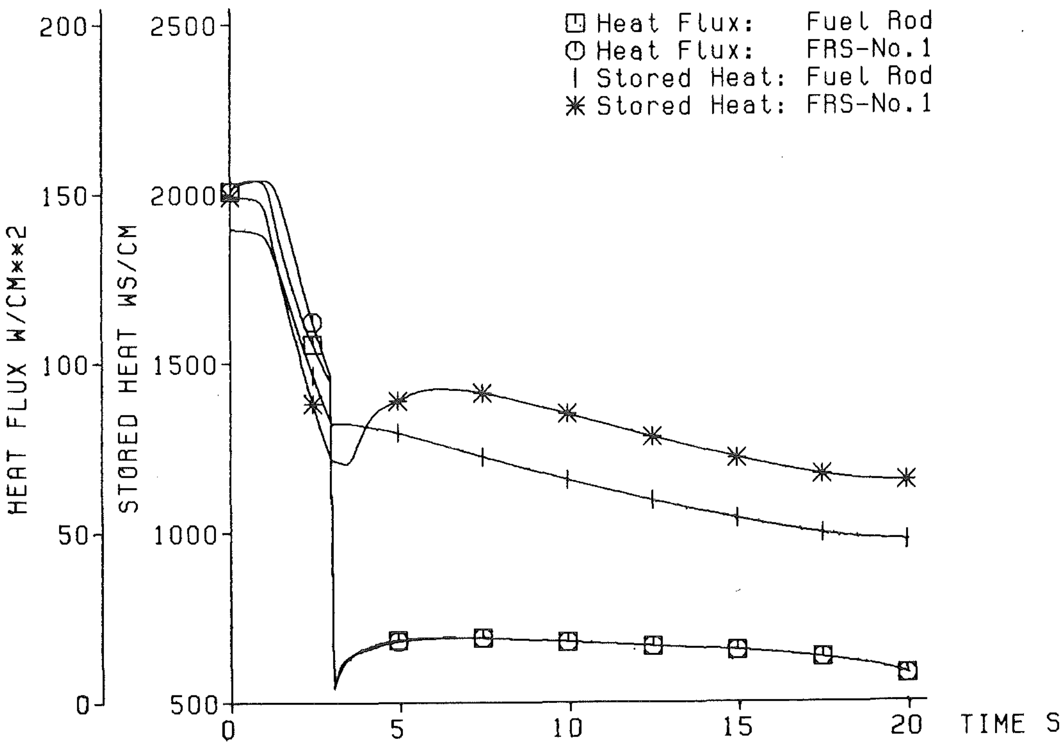

Fig. 15 Thermal behavior of rods achieved by modifying heater rod power

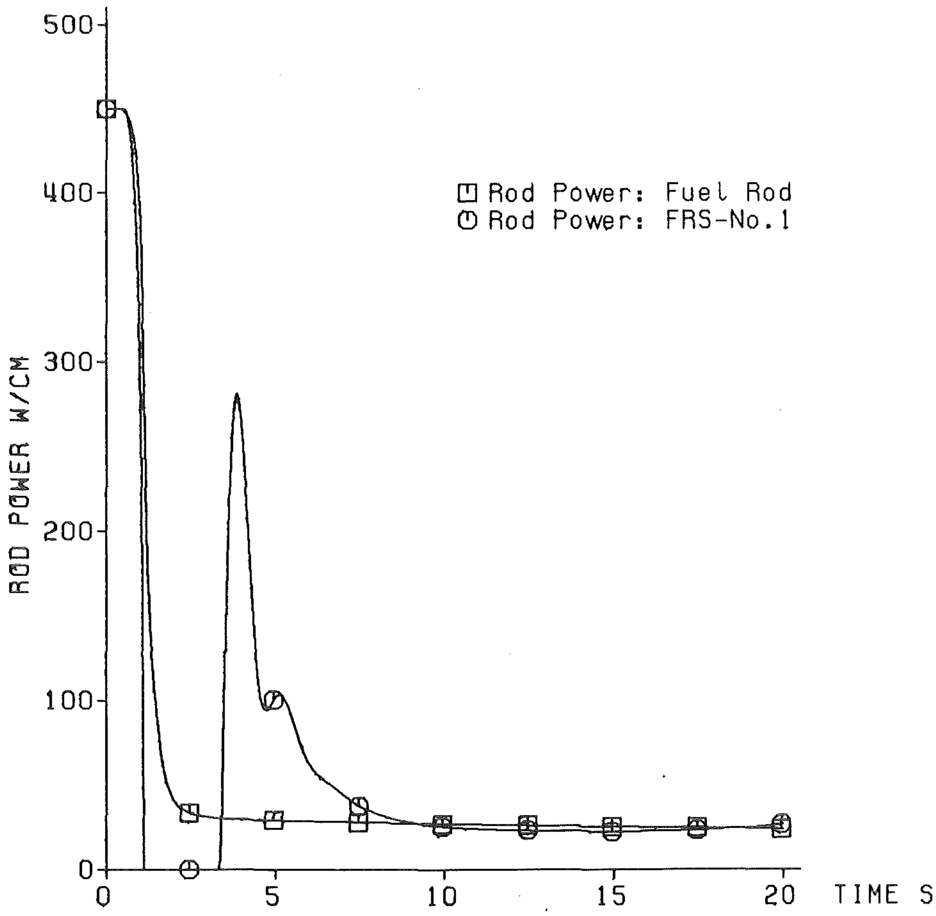

Fig. 16 Fuel rod power and modified heater rod power

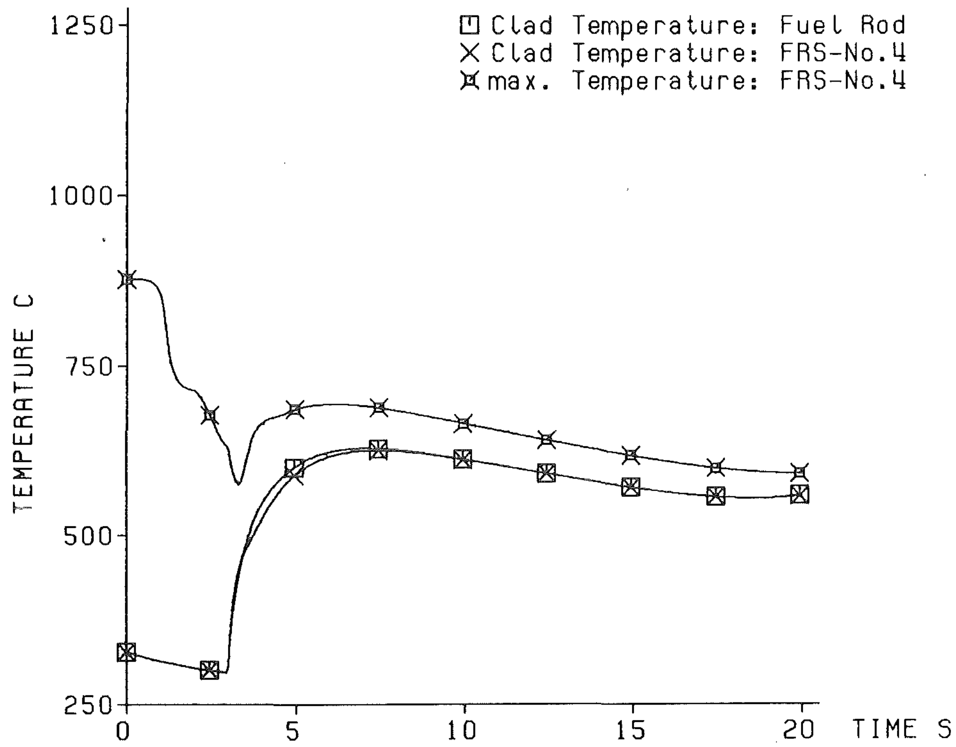

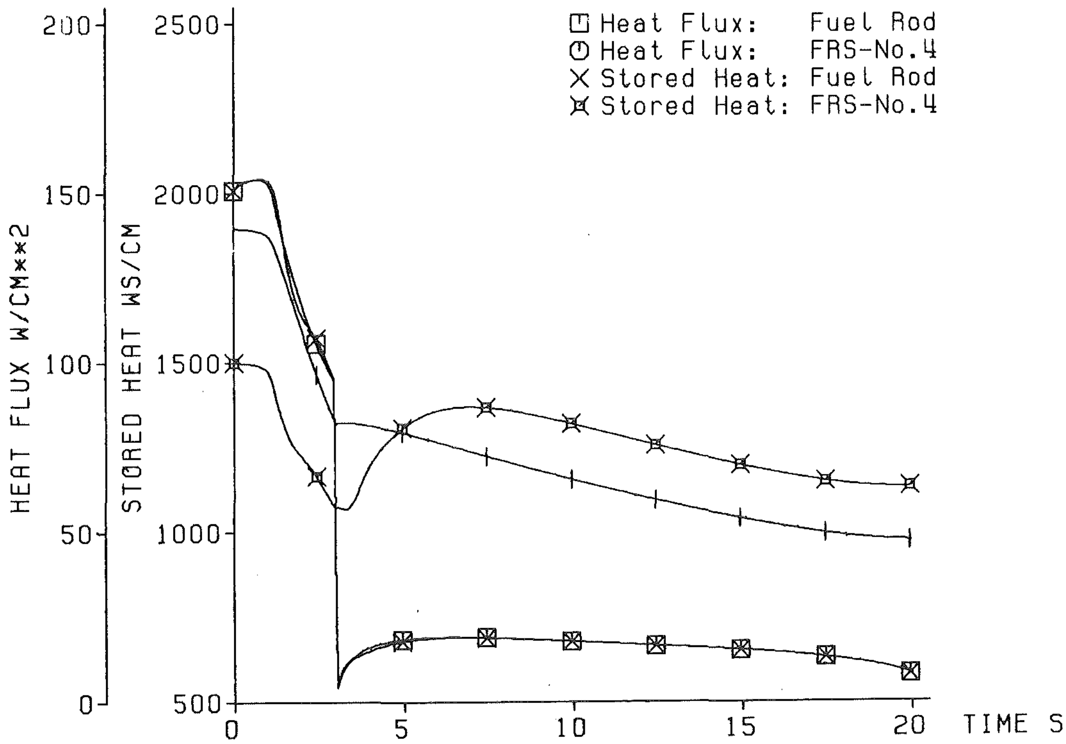

Fig. 17 **Thermal behavior of rods achieved by modifying heater rod power**

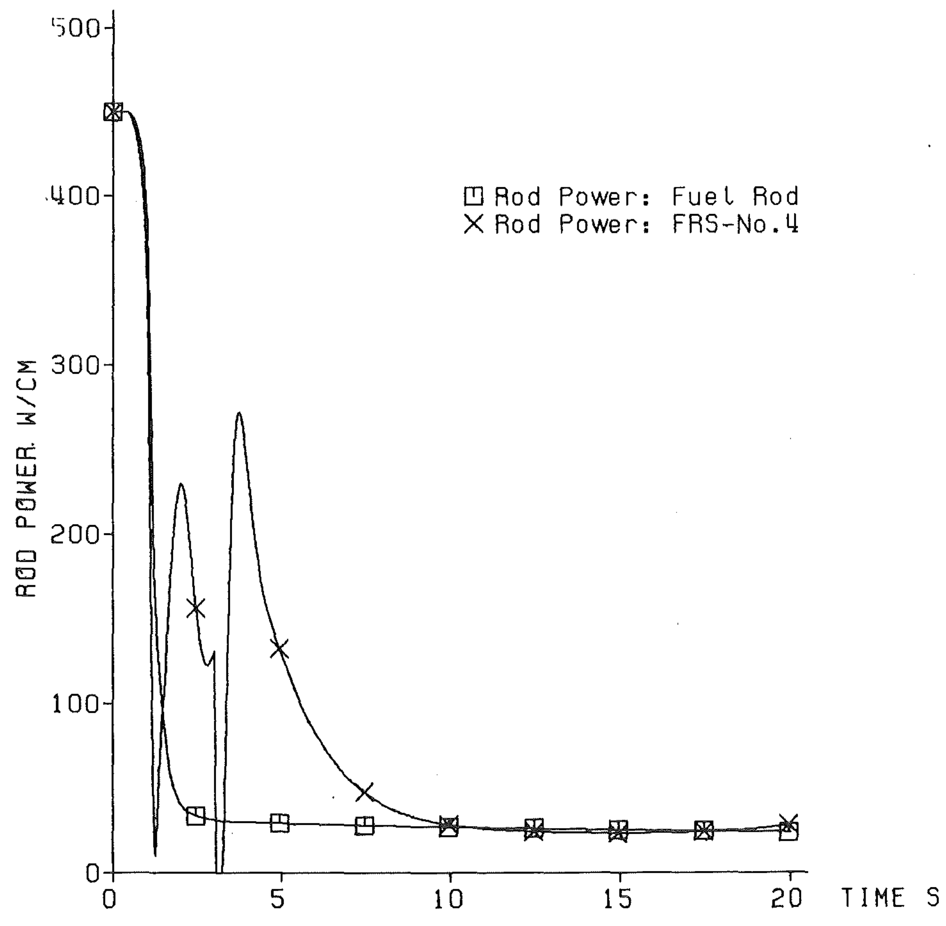

Fig. 18 Fuel rod power and modified heater rod power

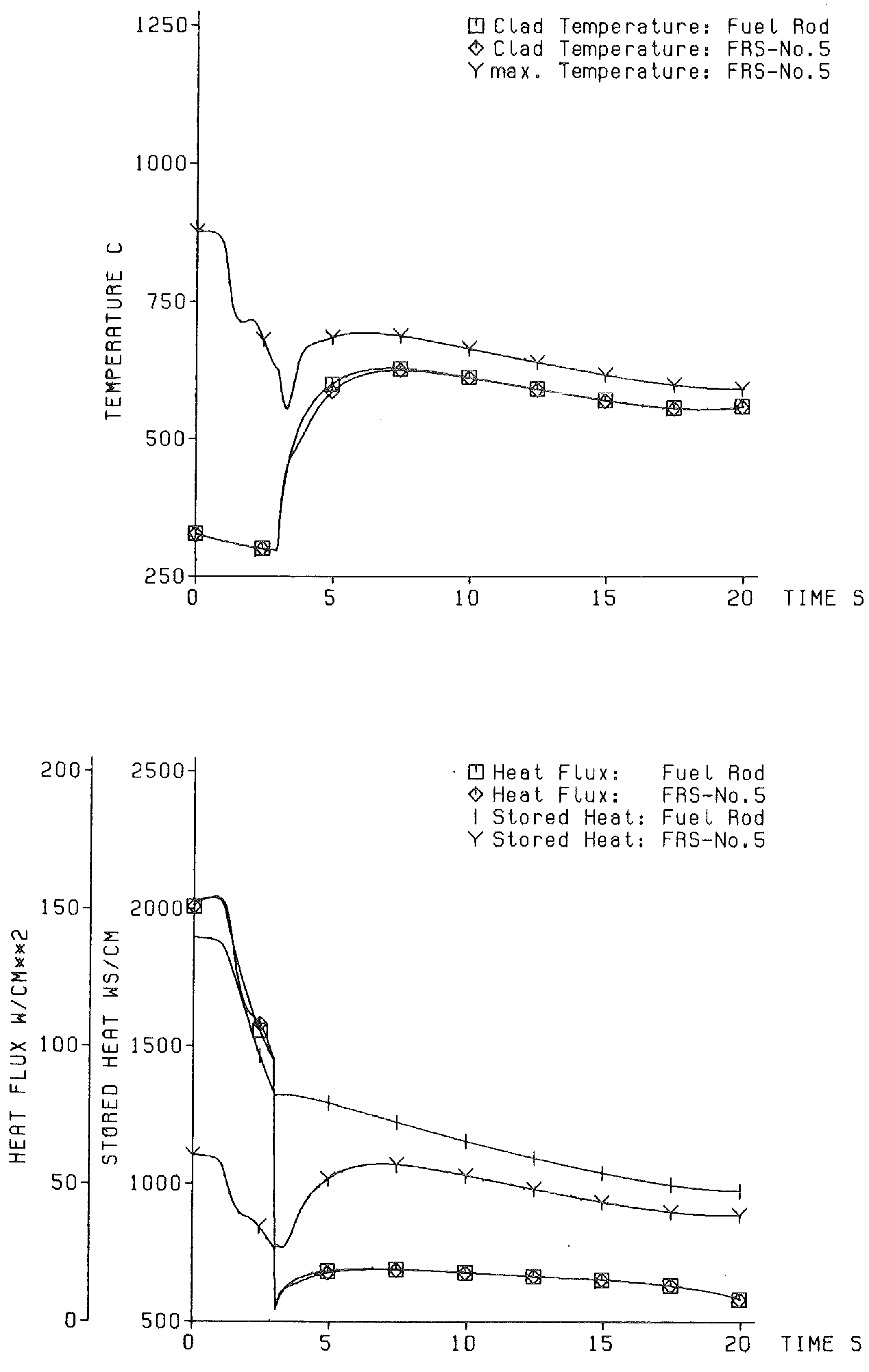

Fig. 19 Fuel rod power and modified heater rod power

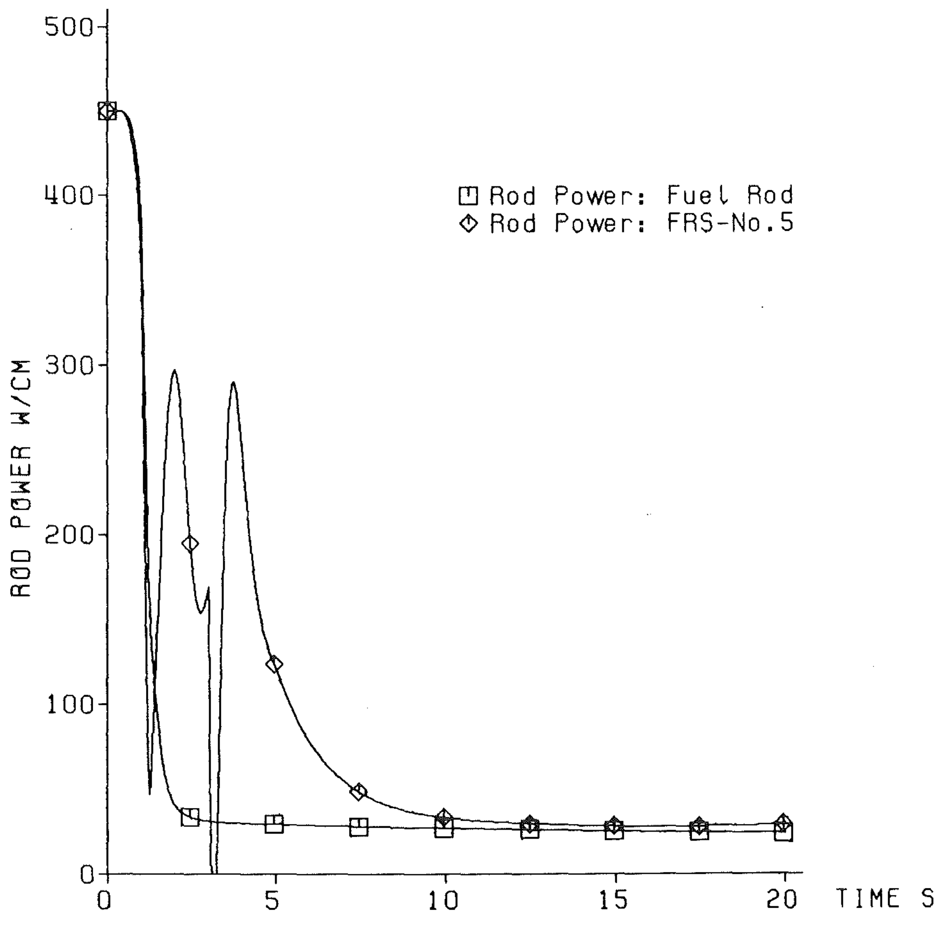

Fig. 20 Fuel rod power and modified heater rod power

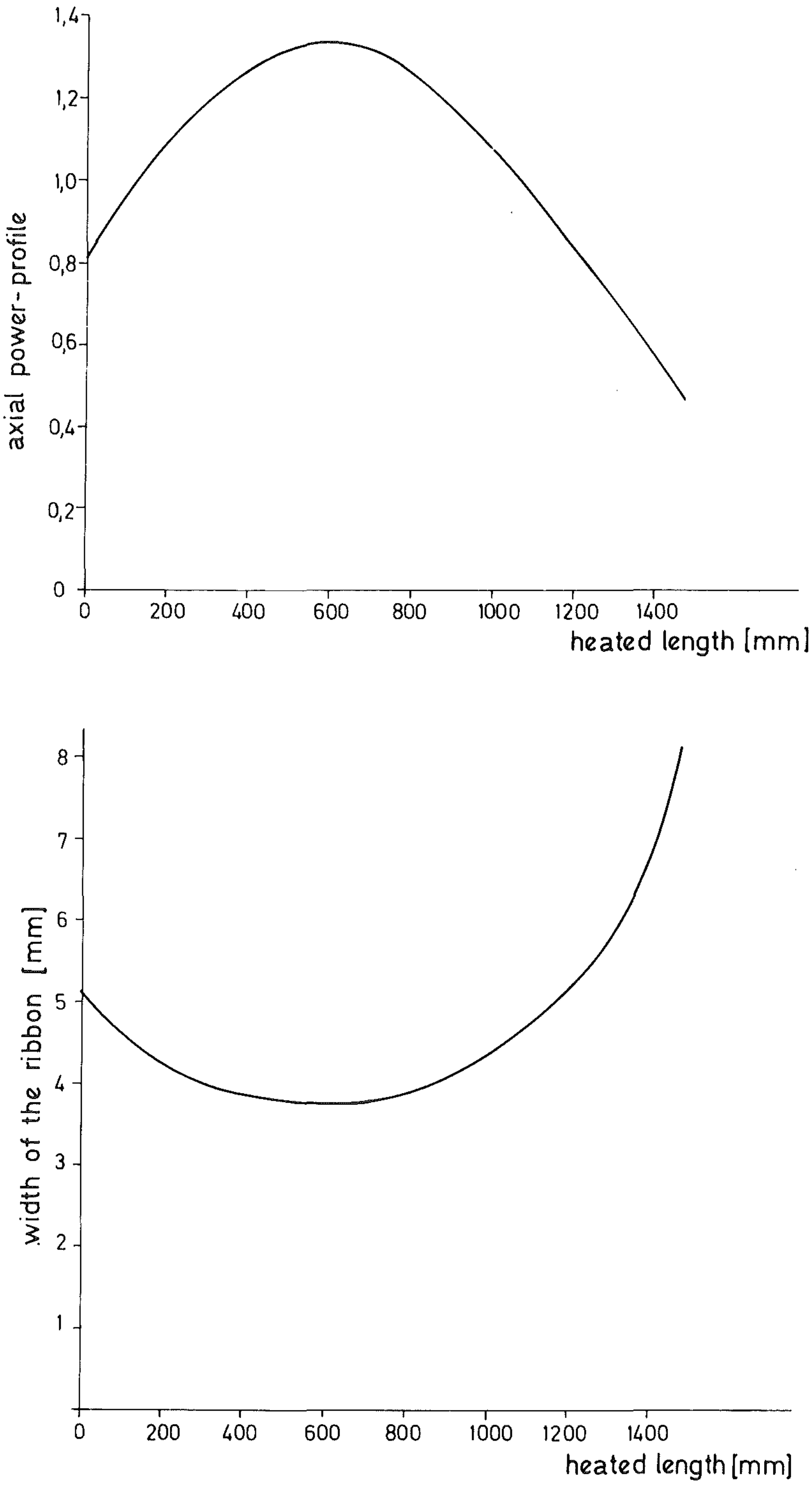

Fig. 21 Axial power profile of HALDEN - reactor and corresponding width of helical conductor of a fuel rod simulator

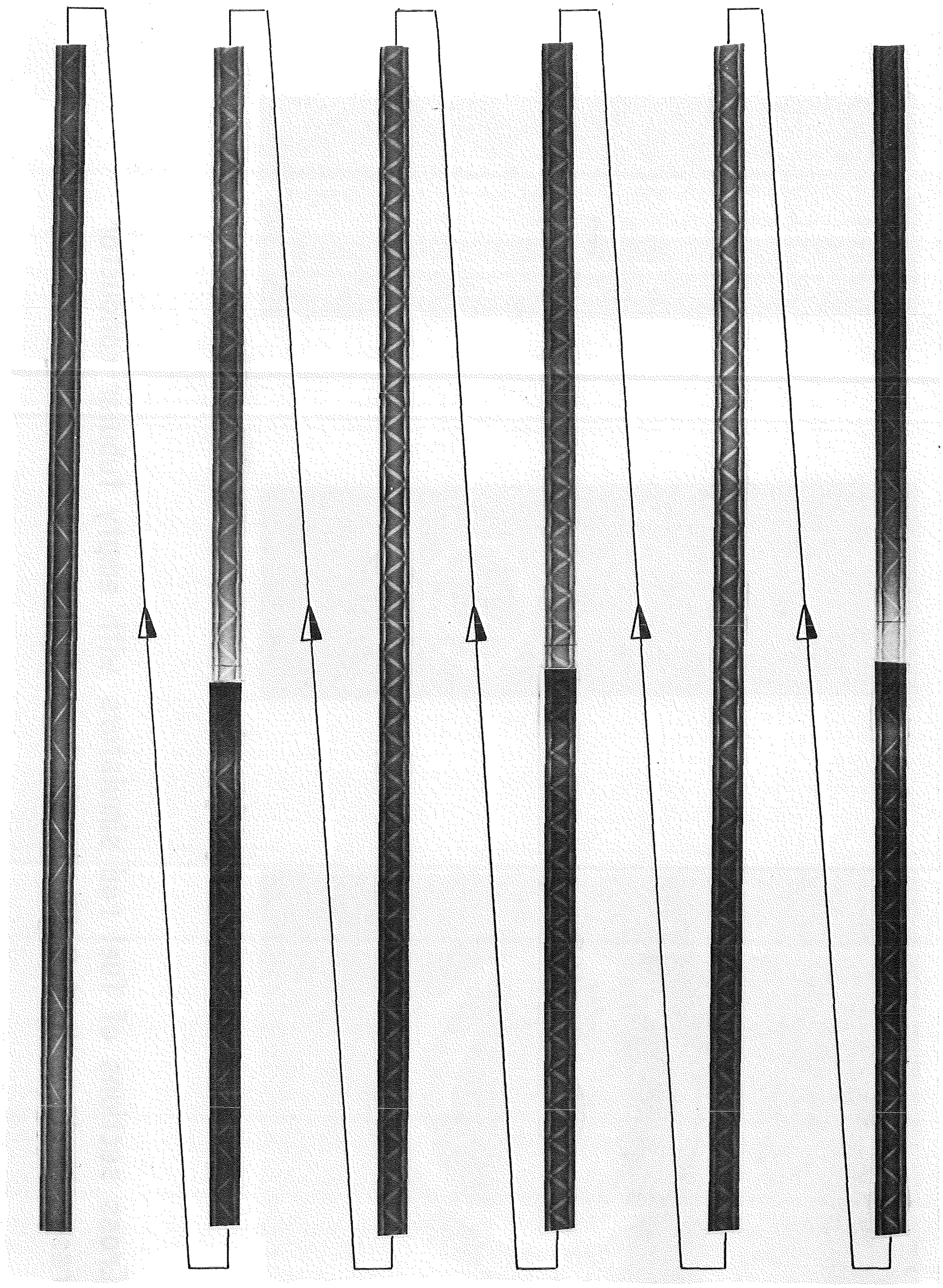

Fig. 22 Radiograph of a fuel rod simulator with helical conductor of variable width

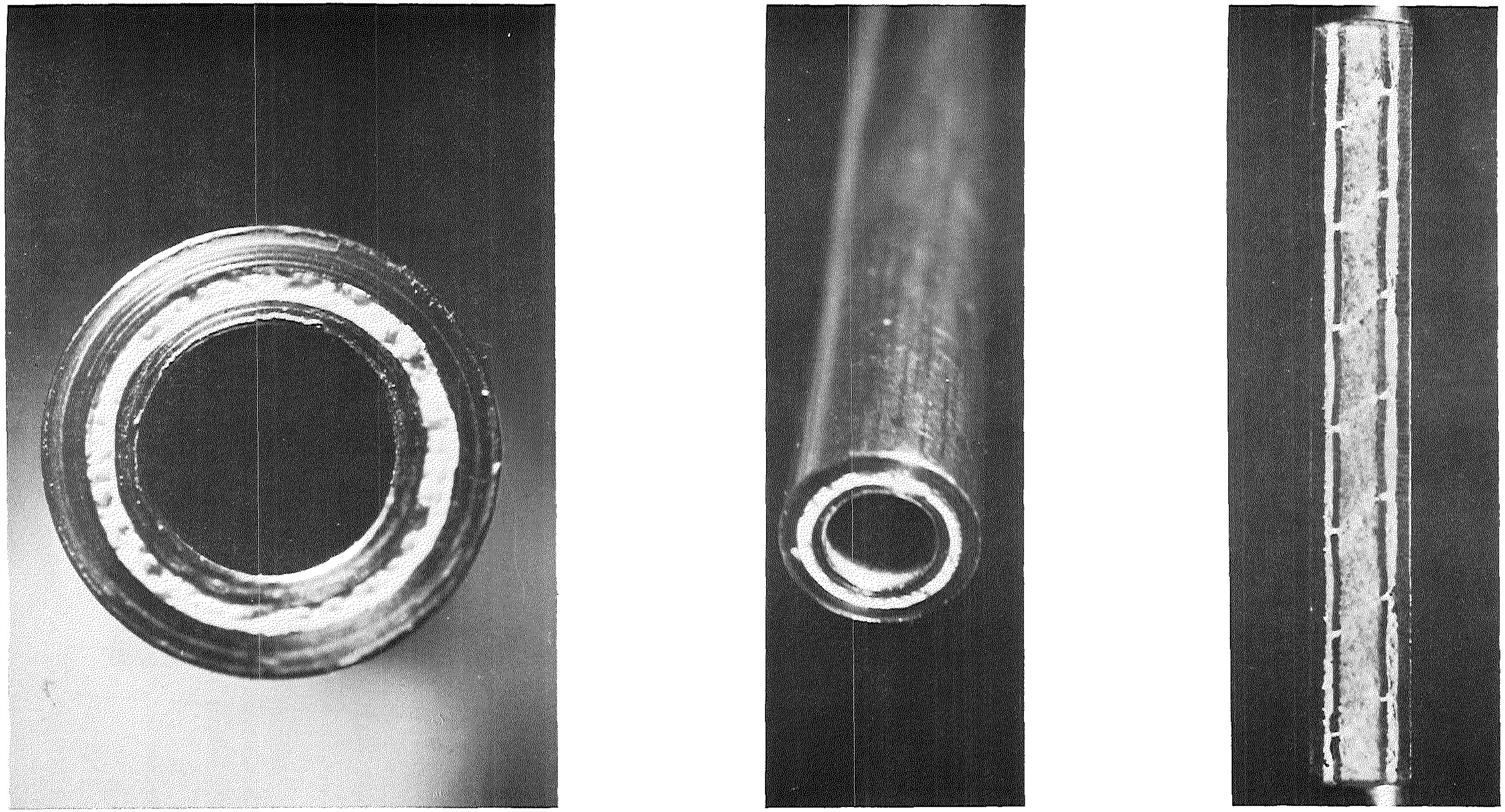

Fig. 23 Cross sections of fuel rod simulators with empty tubular conductor respectively with MgO filled helical conductor